IEEE Access
Multidisciplinary ⋮ Rapid Review ⋮ Open Access Journal

Received November 10, 2020, accepted November 25, 2020, date of publication December 14, 2020,
date of current version December 31, 2020.

Digital Object Identifier 10.1109/ACCESS.2020.3044832

Field I-V Curve Measurements Methodology at String Level to Monitor Failures and the Degradation Process: A Case Study of a 1.42 MWp PV Power Plant

LUÍS GUILHERME MONTEIRO[1,2], WILSON NEGRÃO MACÊDO[3], RENATO L. CAVALCANTE[3], WILSON BRAGA JÚNIOR[3], PEDRO FERREIRA TORRES[3], THIAGO R. BRITO[3], (Member, IEEE), MÁRCIO MELQUIADES SILVA[4], BRUNO MARCIANO LOPES[5], JULIANO M. FRAGA[5], DANILO DERICK ALVES[5], OTÁVIO A. CHASE[6], (Senior Member, IEEE), AND WALLACE C. BOAVENTURA[1], (Member, IEEE)

[1]Graduate Program in Electrical Engineering (PPGEE), Escola de Engenharia, Federal University of Minas Gerais (Universidade Federal de Minas Gerais), Belo Horizonte 31270-901, Brazil
[2]Instituto Politécnico, Pontifical Catholic University of Minas Gerais (PUC Minas), Belo Horizonte 30535-901, Brazil
[3]Group of Alternative Energy Studies and Development (GEDAE), Federal University of Pará, Belém 66075-110, Brazil
[4]Federal Center of Technological Education of Minas Gerais, Belo Horizonte 30720-060, Brazil
[5]Companhia Energética de Minas Gerais (CEMIG), Belo Horizonte 30190-924, Brazil
[6]Cyberspatial Institute (ICIBE), Amazonian Federal Rural University, Belém 66077-830, Brazil

Corresponding author: Luís Guilherme Monteiro (luis.monteiro@gmail.com)

This work was supported in part by the research grants from the Call Nº 13 of an Research and Development Technology Program of electricity sector regulated by the Electrical Energy National Agency (ANEEL), in part by the Companhia Energética de Minas Gerais (CEMIG) through the CEMIG-D Projeto P&D0722—Análise de Arranjo Técnico e Comercial Baseado em uma Planta Piloto de Sistema Distribuído de Armazenamento de Energia em Alimentador Crítico da Rede de Distribuição de 13.8 kV, in part by the Pró-Reitoria de Pesquisa (PRPq) da Universidade Federal de Minas Gerais, in part by the Coordenação de Aperfeiçoamento de Pessoal de Nível Superior / Coordination for the Improvement of Higher Education Personnel (CAPES), in part by the Conselho Nacional de Desenvolvimento Científico e Tecnológico / National Council for Scientific and Technological Development (CNPq), and in part by the Fundação de Amparo à Pesquisa do Estado de Minas Gerais / Research Support Foundation of the State of Minas Gerais (FAPEMIG).

ABSTRACT This research shows the methodology results for outdoor characterization by the I-V curves of the PV power generators at the biggest Brazilian rooftop PV power plant mounted at the Mineirão Football Stadium. The experimental results of the methodology were obtained by a measurement campaign using two capacitive loads. This work identified a significant difference when these measurements were extrapolated to standard test conditions (STC) and compared to the rated power data shown on the PV modules' label at strings: between 24.12% to 26.19% lower. Results showed a contribution of soiling in a power reduction of about 6.7% on average. Additionally, it was considered an uncertain method, and AC electrical parameters were monitored. The reference PV module's calibration was carried out with great attention—the measurements were made with the PV device under test (DUT), guaranteeing the same real operating conditions for the reference PV module and the PV string as DUT. This measurement method has allowed a better characterization of the uncertainty associated with the measurement process. Finally, this study demonstrates the importance of investigating the actual power of the installed PV generators and how these measurements are essential to guaranteeing energy production following the owner's expectations.

INDEX TERMS PV power plants, on-site I-V curve measurements, uncertainty method, translation to STC, commissioning/quality assurance, dust and soiling degradation taxes on PV modules.

I. INTRODUCTION

As the number of big PV power plants increases worldwide, followed by consequent cost reductions, the understanding of PV commissioning is a vital task for the industry, and it is critical to maintaining public confidence and goodwill in such applications [1]–[3]. PV generators' real output power has an essential role in the energy yield, which is the purpose of commercial projects.

The associate editor coordinating the review of this manuscript and approving it for publication was N. Prabaharan.

Commissioning is a means of formalizing the quality control of established PV systems. It is the process of assuring that a PV plant is safe, meets design objectives and functions, and produces energy under the owner's expectations [1], [2], [4]–[6]. It inspires PV integrators to be responsible for their installations and simplifies project closeout and quick payment. Effective commissioning leads to satisfied installers, employers, and PV system proprietors [7]–[9].

One of the helpful tools used in the commissioning process is to carry out on-site I-V curve measurements of photovoltaic strings or generators to assess the PV generator's effective peak power. It also has other advantages such as: testing a vast sample of PV modules right where they are installed, revealing weak PV modules (i.e., hotspots), detecting faulty connections (preventing fire, shocks, and injury), identify shadowing, reverse polarization, and, if done regularly; it may also reveal degradation issues as described by [1], [2], [7], [10]–[12].

The demand for investors for the determination of on-site PV power is increasing [2], [10]–[12]. Brief testing time, low uncertainty, and repeatability of results are critical aspects of the general quality guarantee procedures required to fulfill this demand, as noted in [4], [5], [13]. The market and research laboratories offer various kinds of field I-V curve measurement devices and methods [1], [2], [7], [10], [11], [14], [15] that promise to fulfill these requirements.

According to [1], [2], [10], reliable on-site I-V curve measurements require an operator with good knowledge about the main parameters that influence the measurements. Therefore, an experienced operator is vital because the measurements do not depend only on the I-V curve plotter and the implemented correction procedure (i.e., extrapolation to standard test conditions (STC) or photovoltaics for helpfulness scale applications test conditions (PTC)) [11], [14], [15]. Significantly, the integrator is aware of the specific uncertainties of his/her PV system, and the correct procedure is applied [1], [2], [10], [11], [16].

Although indoor PV module characterization through solar simulators has become further common than outdoor tests under natural sunlight, there are disadvantages to this practice, such as the high costs of solar simulators and a limited number of specialized laboratories to carry out these tests in developing countries such as Brazil.

According to [16], the price of a solar simulator type "A + A + A +" can easily exceed EUR 150,000. This simulator is a huge solution for many PV practitioners (engineers, universities, and other PV professionals) attempting to measure PV modules accurately and control the power provided by PV modules under due diligence.

Outdoor testing is a useful tool for the accurate measurement of PV electrical performance in many developed countries like Brazil. Even with the recent expansion of photovoltaic plants in their electrical networks, these countries still have few specialized laboratories to perform the photovoltaic module's characterization.

Measurement of PV generators on-site is a well-established and well-used commissioning procedure [1], [2], [10]–[13], [16]–[20]. Therefore, the methodology used in this work consists of successive measurements of the I-V curves on PV strings (device under test (DUT)) installed in different segments of the PV power plant. The measures were obtained under natural sunlight conditions, using a non-commercial capacitive load (a self-made capacitive load) and a commercial capacitive load alternately, later extrapolated for STC. Therefore, it was possible to identify each measured string's real rated power and compare the results obtained by both capacitive loads.

Monitoring methodologies are crucial to improving the efficiency of PV power plants. Some researchers have performed studies at the Mineirão PV power plant.

Fraga *et al.* presented in [21] a study to evaluate the impact of PV module dirtiness in the performance of a PV power plant at Mineirão Football Stadium in the Minas Gerais Brazilian state. The authors investigated the dust and soiling events that may cause adverse effects on the PV modules' performance and physically and chemically characterized the dust. The collected dust was mostly made of quartz, hematite, and calcite. These results emphasize the necessity for manually cleaning the PV modules to keep a high generation performance. The particle size distribution and the particle shape were also examined. Regarding the sets of PV modules and the testing period analyzed, soiling reduced peak power by nearly 13.7% in the dry period and 6.5% after a rainfall period. The energy production was reduced by approximately 16.5% in the dry period and 8.0% after a rainfall period.

Monteiro *et al.* presented in [22] outcomes of a one-year monitoring campaign of AC side electrical parameters for the characterization of solar radiation area at the most giant rooftop PV Power Plant, with an installed capacity of 1.42 MWp, installed at Mineirão Football Stadium (Brazil). The authors showed how important it is to survey and characterize the solar resource in the stadium area, based on historical data, to understand solar radiation and design PV power plants with better performance. The findings over the monitoring period were satisfactory, pondering the specificities of the stadium.

Pereira *et al.* presented in [23] a study to estimate the harmonic current contribution as a function of the background harmonic voltage components. Time-domain simulations based on detailed and average models were compared with the frequency domain's impedance model. In grids with harmonic voltages, impedance models can predict the current distortion for all active power injection scenarios. Furthermore, the authors conducted measurements in a 1.42 MW_p PV power plant (at Mineirão Football Stadium in Brazil) connected to a distributed grid, which was used to prove the simulation based on impedance models during different power injections and harmonic voltage profiles. The presented results reinforce the fact that impedance models can represent with relative accuracy the harmonic current

emitted by the PV power plants at the point of common coupling (PCC).

The works cited above [21]–[23] do not specify in detail what level was analyzed for a photovoltaic generation or do not perform a full study of commissioning/quality assurance to compare nominal data with data measured in real operational conditions.

Several works in the literature provide performance assessment of large-scale PV plants. In [24], two similar 100 MW PV plants located in environmentally homogeneous conditions were compared from the monthly AC energy yield perspective, and a significant difference in overall yield was observed during the monitoring period. In this case, the absence of I-V curve measurements prevents an in-depth evaluation of the system, and important factors such as PV modules degradation rate were assumed constant. A performance evaluation of a 10 MW PV plant in India is presented in [25]. The authors obtained data from a SCADA system and evaluated the plant performance using well-known parameters such as the performance ratio, capacity utilization factor, and energy yield. The measured data is compared to software tools' results to evaluate whether the system is properly operating. A 5 MWp PV plant's performance assessment in south India [26] also considered only quantities associated with the plant's energy yield.

Although important, measuring only energy-related quantities do not provide useful information about possible PV modules/arrays inefficient operation. To trace the I-V curve of on-site generators is a way to evaluate its performance deeply. In [12], a 500 kWp I-V tracer was developed for on-site measurement purposes, and the authors concluded that it is a useful tool for the characterization of PV generators and can be incorporated into maintenance procedures. Despite the many advantages of on-site I-V curve tracing, outdoor characterization is more prone to uncertainties associated with measurements and STC (or PTC) extrapolation than indoor solar simulators. A detailed assessment of the uncertainties in outdoor module characterization is presented in [16]. In this sense, a methodology to reduce such uncertainties is vital to guarantee reliable results. The twin capacitive load introduced in [27] is used to simultaneously trace I-V curves for two different PV modules/arrays.

This article took advantage of the twin capacitive load concept to develop a novel methodology to characterize outdoor PV arrays with improved reliability by correcting outdoor measurements to a traceable indoor-calibrated reference PV module. The methodology consists of simultaneously tracing I-V curves for the DUT and a previously calibrated reference module, making it possible to quantify the relative extrapolation error, which is assumed to be the same for both the reference module and the array being tested. Therefore, the proposed methodology makes it possible to evaluate the quality of the extrapolation process. To summarize, the main contributions of this article consists in: first, the demonstration that an outdoor characterization is a crucial tool in large scale PV assessment by presenting a detailed procedure and insightful results; second, the novel methodology that consists in the application of the twin capacitive load concept to evaluate the quality of the extrapolation process.

This article presents the results of the on-site I-V curve measurements at the string level in a 1.42 MWp PV power plant located at Mineirão Football Stadium's rooftop. Significant differences between nominal and measured data are considered evidence of the importance of this type of assessment. Furthermore, the results provide simultaneous measurement information on a reference PV module, calibrated with a solar simulator of type "A + A + A +" (one of the best on the market), and the devices under test. This aspect helps measure uncertainty in evaluation even outside the irradiation range restricted by IEC 60891 [28].

The following sections describe the PV power plant system, the methods used to perform I-V curve measurements, and the uncertainty calculations. An analysis of the results found is presented in the final section.

II. MINEIRÃO FOOTBALL STADIUM POWER PLANT

Mineirão Stadium, officially named *Estádio Governador Magalhães Pinto*, was started in 1965 and is in the north region of the city of Belo Horizonte, capital of Minas Gerais State, in Brazil, at latitude 19°′5157″ S and altitude 43°58′15″ W. In the years 2013, 2014, and 2016, the stadium hosted games of the FIFA Confederations Cup, FIFA World Cup, and Rio Summer Olympic Games. Therefore, Mineirão is considered one of Brazil's most famous football stadiums.

After Brazil won the bidding to host the World Cup in 2014, Mineirão had a massive redevelopment/retrofit. A 1.42 MWp, PV power plant was installed on the stadium's rooftop as a part of its modernization efforts [29]. This PV system is the largest rooftop PV installation in a football stadium in Brazil and presents challenging conditions regarding optimal system performance achievement, as described below.

The PV power plant comprises 5910 poly-crystalline silicon PV modules, model Mprime (Martifer) model M 240P. The 360° rooftop is partitioned into 88 physical segments with 42 segments (21 east and 21 west regions) containing 75 PV modules each (18 kWp/segment) and 46 segments (23 north and 23 south regions) with 60 PV modules each (14.4 kWp/segment).

All PV modules that comprise each physical segment have a tilt of 8°, following the roof inclination angle. The PV modules may not appear to the public due to restrictions on the stadium's structures from being changed (imposed by the agency that grants to buildings the title of Cultural Heritage of the Municipality). This restriction to installing the photovoltaic generator arrays culminated in shading problems on the arrays' plane throughout the year. [16]–[18].

Each segment comprises 6 or 7 chains (9 or 12 PV modules, each chain) connected to an inverter model Ingecon Sun Smart TL (manufactured by Ingeteam). This inverter has a nominal power of 15 kW and includes three maximum power point trackers (MPPT) (2 or 3 chains for each MPPT).

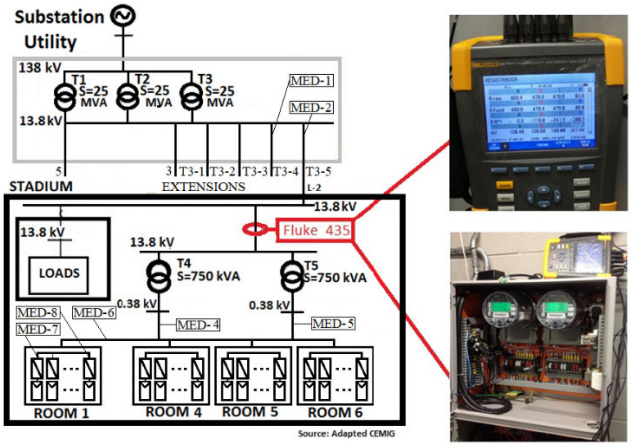

FIGURE 1. The utility grid interface diagram with the PV power plant indicates the installation of the Fluke 435 energy analyzer.

FIGURE 2. (a) Aerial view of the stadium with 1.42 MWp PV generator installed on the rooftop and string installation detail; (b) detail of PV module arrays (strings); (c) scheme of eight inverter room and substations sectors "A" and "B"; (d) PV plant/utility grid connection substation; (e) step-up substation (380 V to 13.8 kV); and (f) PV plant/utility grid main switchgear.

Therefore, 88 inverters compose the whole system in the stadium, to a total nominal inverter power of 1.32 MW.

Each inverter is connected to a 380 AC voltage (phase to phase) supplied by two 750 kW electrical substations that step-up the voltage to a 13.8 kV bus for the distribution system. Figure 1 shows a unifiliar diagram with a data acquisition device (Fluke 435) connected to the point of common coupling (PCC) with the utility grid. Figure 2 shows an aerial observation of the stadium with the 1.42 MWp PV generator rooftop, an overview of the whole system. More details on this installation can be found in [22], [30], [31].

III. MINEIRÃO PV GENERATOR CHARACTERIZATION PROCEDURE (MATERIALS AND METHODS)

A. MEASUREMENT CAMPAIGN

For the measurement campaign, two capacitive load devices were used. One (with two capacitors: 0–500 Vdc ± 0.5%, 0–20 Adc ± 0.5%; 0–50 Vdc ± 0.5%, 0–10 Adc ± 0.5%) that was developed by the Group of Alternative Energy Studies and Development (GEDAE) from the Federal University of Pará (UFPA) in Brazil, which can measure on-site I-V curves from PV generators and a reference PV module simultaneously. The other is a capacitive load manufactured by Solmetric (commercial), model PVA 600 (600 Vdc ± 0.5%/20 Adc ± 0.5%).

The first capacitive load device performs simultaneous measurements through two capacitors. The objective of using two capacitors for simultaneous measurements is to compare the results obtained from the extrapolation method for photovoltaic generators under test and for a photovoltaic reference module that has been previously calibrated in a solar simulator (with quality characteristics two-times better than the best class A, established by IEC 60904-9 [32]).

Additionally, it is possible to obtain data on environmental conditions during measurements without using any sensor. Both the irradiance and temperature of the PV generator can be calculated using the short-circuit current (I_{sc}) and open-circuit voltage (V_{oc}) of the reference PV module, respectively. In this case, the photovoltaic reference module's temperatures and the photovoltaic generator under test are the same. Such an assumption is most accurate if the reference PV module has the same technology (or, even better, if it is the same model) as the PV module that comprises the PV generator being tested [16].

To measure the current (I) and voltage (V) parameters in the GEDAE capacitive load, a scopemeter from Fluke model 190–504 series II (four-channels) was used. This equipment has four channels that can measure many electrical parameters such as voltage (Vacrms, Vdc, Vac+Vdcrms until 1000 V ± 1.5% Vnominal/Vdc ± 0.5%), current (0.5 A to 1000 A, DC ± 0.5%), power (W, VA, Var, W).

To size the capacitor, the photovoltaic generator is considered to behave as an ideal current generator. Thus, the voltage of the capacitor increases linearly until it reaches the open-circuit voltage in a load time, t_C, which can be calculated by Equation (1):

$$V_G(t) = \frac{I_{SC}t}{C} \Longrightarrow V_G(t = t_C) = V_{OC} = \frac{I_{SC}t}{C} \Longrightarrow t_C = \frac{V_{OC}C}{I_{SC}} \quad (1)$$

C is the capacitor's capacitance, and the V_{OC}/I_{SC} ratio is known as the specific resistance of the generator. The current decreases as the voltage increases, which implies that the charging time will be longer than that calculated by Equation (1). However, the error caused by this approach does not compromise the design stage of the load since the load time depends on the specific resistance of each photovoltaic generator, and, for sizing, it is advisable to adopt values between 20 and 100 ms.

The GEDAE capacitive load used a 22 Wp c-Si PV as a reference module, calibrated on a Pasan "A + A + A +" class solar simulator at GEDAE/UFPA, and that was used as

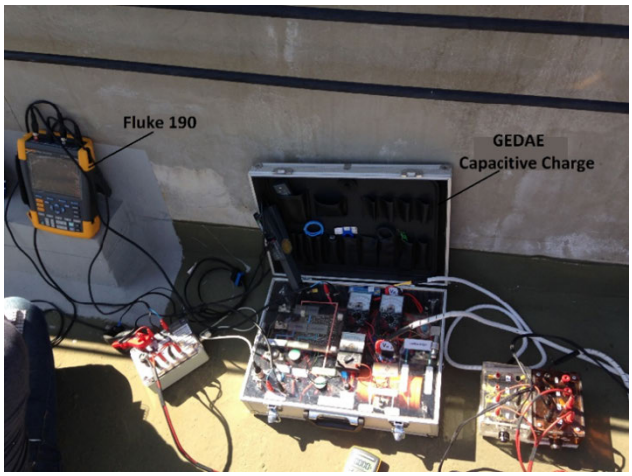

FIGURE 3. Group of Alternative Energy Studies and Development (GEDAE) double capacitive load (charge) coupled with the four-channel Fluke 190.

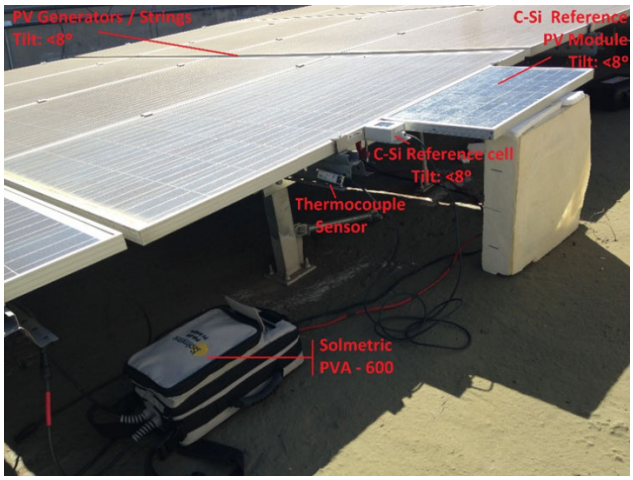

FIGURE 4. The c-Si solar PV cell and PV module (coplanar to the PV generator), thermocouple sensor, and Solmetric (PVA 600) commercial capacitive load.

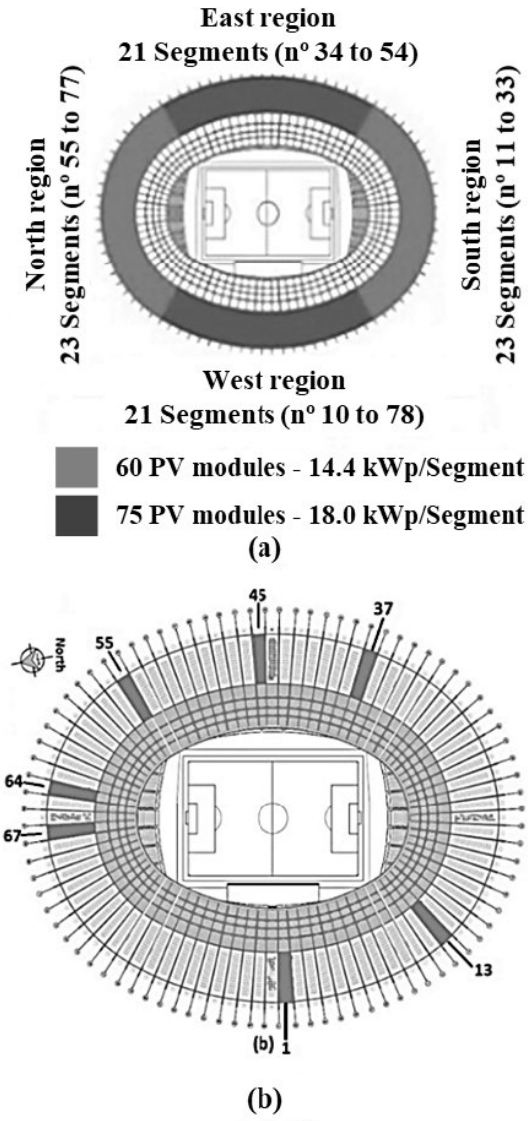

FIGURE 5. PV detail of module arrays: (a) 88 segments with a different number of PV modules, (b) location of chosen segments (dark grey rectangles).

a primary calibrated sensor. For the commercial capacitive load, a c-Si reference cell was used (with corrections for temperature, spectral, and angular effects, accuracy $\pm$ 2%, used as a secondary calibrated sensor). Additionally, the Solmetric wireless sensor kit was used for data acquisition with thermocouples type K, with two inputs attached to the back of PV modules (accuracy $<$ 2 °C, including inherent thermocouple limitations/0.1 °C resolution).

The reference PV cell and the PV module were attached at the same plane (with a tilt of 8°) and orientation as the PV generators (string). Figure 3 shows the GEDAE capacitive load coupled with the Fluke scopemeter 190. Figure 4 illustrates the c-Si reference PV cell/module (coplanar to PV generator), the thermocouple sensor, and the Solmetric (PVA 600) commercial capacitive load.

The measurement campaign lasted five days (between 11 and 15 July, during the winter season of 2016), from 9:30 a.m. to 01:30 p.m., and it monitored seven segments of the PV power plant, with 6–7 strings/segment (9–12 PV modules/string).

Measuring small system parts gives a closer look at the PV modules, so one or two PV strings (PV1/PV2) per segment were chosen for several measurements (on average, ten measurements/PV string). Table 1 shows the chosen segments' numbers and characteristics of the chosen PV strings. Figure 5 illustrates the localization of the chosen segments (dark grey rectangles), and Figure 6 gives details (zoom) of the PV1 (black rectangles) and PV2 (gray rectangles) strings/number of PV modules.

Usually, the surface of PV generators accumulates soiling and dust over time. One PV module at the PV1 generator in segment 13 was randomly chosen to be cleaned to acquire an I-V curve measurement without the interference of soiling and dust and hence receive a reference measurement for comparison and analysis. Figure 7 illustrates the clean PV module.

TABLE 1. Segment numbers and characteristics of chosen PV generators.

Location	Segment Number	PV 1 Number of Modules Per String (String Peak Power)	PV 2 Number of Modules Per String (String Peak Power)
North side	64	10 (2.4 kWp)	10 (2.4 kWp)
North side	67	10 (2.4 kWp)	10 (2.4 kWp)
Northeast side	55	10 (2.4 kWp)	10 (2.4 kWp)
East side	45	09 (2.16 kWp)	09 (2.16 kWp)
East side	37	09 (2.16 kWp)	09 (2.16 kWp)
West side	01	09 (2.16 kWp)	09 (2.16 kWp)
Southwest side	13	10 (2.4 kWp)	10 (2.4 kWp)

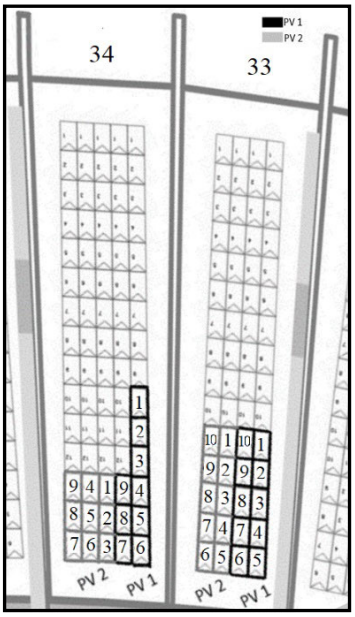

FIGURE 6. Example (zoom) of the PV1 (black rectangles)/PV2 (grey rectangles) generators, number of PV modules.

B. MEASUREMENT METHODOLOGY

PV modules and the estimation of its uncertainties on STC power measurement have gained awareness in recent years and seen some enhancements [1], [2], [16]. For uncertainty estimation, stability issues must be contemplated in addition to pure measurement uncertainty: STC power is often not a constant value, but dependent on preceding exposure to light and temperature. For energy rating, the STC power is essential (representative of field operation) [1], [2], [52].

In this work, string measurements were translated into STC by applying mathematical procedures [1], [2], [10], [18], [33]–[38] for temperature and irradiance correction. Therefore, the actual STC power is derived from measurements and correction described by [2], [10], [33]. Figure 8 shows these two steps for the characterization of the string output power based on outdoor measurements.

As Figure 8 illustrates, both steps are affected by uncertainties regarding the measuring process (U_{meas}, step 1—introduced by the equipment and its traceability

FIGURE 7. Cleaning of the PV module.

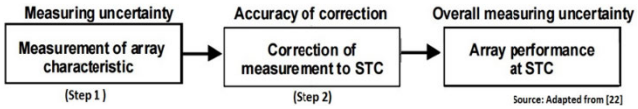

FIGURE 8. Steps for characterization of the PV array performance [10]. STC: standard test conditions.

chain) and the accuracy of the translation (U_{corr}, step 2). The latter is composed of the model's capability to describe the module behavior, the uncertainty of the model parameters in use, and the environmental measurement conditions. Therefore, the uncertainty introduced by the correction will be lower when the real conditions are closer to the STC [1], [2], [10], [16], [33]. Ultimately, the results of the two steps result in overall uncertainty (U_{tot}).

Method one was used for this work: an algebraic procedure, proposed by IEC 60891 [28] to perform the on-site data translation into STC. Equations (2) and (3) show the correct equations.

$$I_{STC} = I_m + \left(\frac{1000\frac{W}{m^2}}{G_m} - 1\right) x I_{SC,m} + \alpha\left(Tc - 25^{\circ}C\right) \quad (2)$$

$$V_{STC} = V_m - R_s\left(I_{STC} - I_m\right) - K x I_{STC}\left(T - 25^{\circ}C\right) + \beta\left(Tc - 25^{\circ}C\right) \quad (3)$$

where: V_m is the voltage, I_m is the current, G_m is the irradiance, and T_c is the cell's temperature. Subscript m stands for measured quantity, and subscript STC for the quantity corrected to STC, α is the temperature coefficient for short circuit current, β is the temperature coefficient for open-circuit voltage, K is the curve correction factor, and R_S is the series resistance.

The overall uncertainty was calculated using the law of error propagation cited in the literature [37], [38], [39]–[44]. By applying this methodology to the correct equations (Equations (2) and (3)) and, according to

the type B method as proposed by JCGM/GUM [41], Equations (4) and (5) calculate the combined uncertainty of the corrected power ($U_{P,STC}$).

$$U_{P,STC} = \sqrt{\sum_i^n u_{x_i}} \tag{4}$$

With

$$u_{x_i} = \left(\frac{\partial P_{STC}\left(x_i, \ldots, x_n\right)}{\partial x_i} \right)^2 \Delta x_i^2 \tag{5}$$

where: P_{STC} corresponds to the voltage and current at the maximum power point in STC ($V_{MPP\ -\ STC}/I_{MPP-\ STC}$). According to Equations (4) and (5), x_i represents all the measured quantities and parameters needed to determine P_{STC}.

According to [1], [2], [10], [15]–[17], [43], [44], the significant relative contribution to the uncertainty of the PV module or the entire PV generator/string power rating results comes from the calibration of the reference device (PV cell and PV module) used to obtain the incident irradiance. The irradiance must be typically restricted to the range between 800 and 1100 W/m^2 to reduce the I-V curve corrections. The measurement of a reference module and DUT at the same time could help reduce this uncertainty, even when the irradiance is out of the recommended range.

Therefore, for this work, the uncertainty calculation for P_{STC} was made as a case study of specific conditions, i.e., when measurements achieved the range described above. Table 2 shows the standard uncertainties and the resulting combined uncertainty in measured irradiance values, according to the reference PV cell and PV module used in this work.

Additionally, it is vital to consider the uncertainty introduced by the irradiance measurement's temperature correction and remember that the closer the reference PV cell temperature is to 25 °C, the lower the uncertainty is. Table 3 illustrates the typical standard and the resulting combined uncertainty of this work's measuring temperature.

The I-V curves of PV1 and PV2 were measured with capacitive loads, so the measurement instruments' choice and their calibration are decisive for uncertainty calculations. Table 4 summarizes the estimated uncertainties for Solmetric and GEDAE capacitive loads.

In Table 4, the measurement combined uncertainties of the I-V curve tracers are closer to manufacturers' considered parameters [45], [46], [50]. Table 5 gives an example of the measurement uncertainties achieved for the PV1 array in segment 64 at 805 W/m^2 and 45 °C using the Solmetric device.

Regarding model parameters α, β, $\mathcal{K}$ (that describe the behavior of a module at different temperatures), and R_S (series resistance), which are necessary for the correction to STC according to procedure 1 in IEC 60891 [28], the parameters suggested by Drnberger *et al.* [10] were used, which analyzed around 120 temperature coefficients measurements and around 80 measurements at different irradiance levels. The standard uncertainties were calculated as the square root of the square sums of the contributing uncertainties. Table 6 illustrates the estimation results of the correction parameter uncertainties for a poly-crystalline (poly c-Si) PV module.

The total contributions (in W) to the combined uncertainty of P_{STC}, i.e., the summands in Equation (3), for an irradiance $\geq$ 800 W/m^{2,} and cell temperature 45 °C are shown in Table 7.

Table 7 shows the result of the combined uncertainty of P_{STC}, 4.0%, which is similar to the one identified by Drnberger *et al.* [10], 4.2%, for the same conditions. Drnberger *et al.* [10] also found values of 3.2% and 6.4% for temperatures of 25 °C and 65 °C, respectively. Therefore, this work considered a mean value of 4.6% from these values for

TABLE 2. The combined uncertainty of measured irradiance for values refer to (A) the reference PV cell and (B) the reference PV module used. DUT: device under test.

(a)	Reference PV Cell	
Standard Uncertainties	**[%]**	**References**
Calibration Value	2	[1,45,46]
Uncorrected calibration value	0.01	[39]
Stability	2	[10]
Shunt	0.15	[45,46]
Temperature @ 40 °C	0.3	[10]
Temperature coefficient	0.25	[10]
Data aquisition	0.03	[10]
Spectral Mismatch	0.8	[39]
Inhomogenity	0.5	[10]
Combined Uncertainty @ 40 °C	**3.01%**	
(b)	**Reference PV Module**	
Standard Uncertainties	**[%]**	**References**
Spectral Match	< ± 0.0125	
Non-uniformity	< 0.01	
Instability	< 0.01	
DUT type	Mono-crystalline Si	
Reference Device	Mono-Si, the same type as DUT	[16,47,48]
Reference Device uncertainty over Isc and Voc	0.016, 0.012	
Maximum incidence angle	15°	
SMM	Considered	
Data acquisition	0.03	
U_c on P_{max} (coverage factor k = 2)	**3.00%**	

TABLE 3. The combined uncertainty of measured irradiance for values refer to (A) the reference PV cell and (B) the reference PV module used. DUT: device under test.

Parameters	Absolute Uncertainty	Standard Uncertainty [%]	References
Thermocouple type K		0.75	[49]
Difference back/junction	0.5 K	0.7	[10]
Temperature inhomogeneity	2 K	2.6	[10]
Data acquisition		0.03	[10]
Combined Uncertainty at 45 °C		**2.80%**	

TABLE 4. Measurement uncertainties of the I-V curve measurement by capacitive loads of (A) Solmetric and (B) GEDAE.

(a) Measurement Uncertainties of the I-V Curve Tracer—Solmetric			
(a)	Standard Uncertainty	Considered [%]	References
Current	<5%	1	[45,46]
Voltage	<5%	1	
Isc	<3%	2	
Voc	<2%	2	
Pmpp	<2%	2	
Combined Uncertainty		3.74%	
(b) Measurement Uncertainties of the I-V Curve Tracer—GEDAE			
(b)	Standard Uncertainty	Considered [%]	References
Current	<5%	0.5	[50]
Voltage	<5%	0.5	
Isc	<3%	2	
Voc	<2%	2	
Pmpp	<2%	2	
Combined Uncertainty		3.54%	

TABLE 5. Measurement uncertainties in the I-V curve measurement using Solmetric load.

The Measurement Uncertainties		
Parameters	Measured Value	Standard Uncertainty
Irradiance	805 W/m^2	3%
Temperature	45 °C	2.80%
Measured Power	1,891 Wp	2%
Measured Isc	7.25 A	2%
Measured Voc	353 V	2%
Combined Uncertainty		5.37%

TABLE 6. Estimated parameter standard uncertainties.

Poly—Reference [10]		
	[%]	[W]
α	35	8
β	11	42
K	34	11
Rs	30	29

measurements equal to or above 800 W/m^2 for irradiance and between 45 °C and 65 °C for the temperature.

It is worth citing that up to now, there is only rudimentary information on individual measurement uncertainties from different laboratories achieved for power measurements at conditions different to STC. A deficiency partly causes this variety of information in demand for such measurements—a typical PV module datasheet contained 2 or 3 power specifications (for STC and 200 W/m^2 at 25 °C, sometimes for 800 W/m^2 at NOCT) and the temperature coefficient of output power only [2].

Nowadays, with higher demands on product characterization and the availability of the IEC 61853 standards on PV module energy rating, more laboratories offer comprehensive power rating measurements, covering a full matrix of irradiance and temperature conditions. Nevertheless, the uncertainty of these non-STC measurements is still more or less unknown [2]. Therefore, each measurement has its own

TABLE 7. The contributions to the combined uncertainty of P_{STC} of all quantities for irradiance ≥ 800 W/m^2 and temperature 45 °C.

Parameter	[%]	[W]
α	35	8
β	11	42
K	34	11
R_S	30	29
I_{mpp}	0.5	25
V_{mpp}	0.5	30
E	3	58
I_{SC}	2	2
T_{array}	2.8	20
$U_{P,STC}$ (k = 1)	N/A	90
$U_{P,STC,\ relative}$ (k = 2)		4%

TABLE 8. Estimated parameter standard uncertainties.

	Uncertainty	Conditions
Lab. 1	some 5%	for extreme temperature/irradiance combinations
Lab. 2	3.6%	with matrix measurements at low irradiance values
Lab. 4	3.2%	at 200 W/m^2 and 65 °C
Lab. 7	3.5%	at 1,000 W/m^2 and 70 °C
Lab. 8	2.2%	at 100 W/m^2 and 75 °C

Source [2]

uncertainty, which depends on the measurement system and weather conditions. Furthermore, indications that give general measurement uncertainties without referring to specific conditions can be interpreted as a minimum value [10]. A few laboratories provided some information on the maximum uncertainty of power measurements at the related conditions, as shown in Table 8.

During the period of the measurement campaign, data from a Fluke 435 were also used. This equipment measures and stores average values of voltage, current, active (P), reactive (Q), and apparent (S) powers, as well as other variables of interest sampled per phase and stored with a resolution time of 5 min (see Figure 1). The data acquisition device was connected to the point of common coupling (PCC) with the utility grid and PV power plant. All data were used during the assessment of the performance of the PV system during the measurement campaign.

Finally, the time and global horizontal irradiation data (GHI) (measured by a CPM 21 from Kipp and Zonen) from the meteorological/solarimetric station of the National Institute of Meteorology (INMET) were also used. This station is installed on the Federal University of Minas Gerais (UFMG) campus, which is located only 2 km from the Photovoltaic Plant of Mineirão.

IV. RESULTS (AND DISCUSSION)

A. MONITORING THE PV POWER PLANT OF MINEIR AO SOCCER STADIUM

As already mentioned, the measurements of the AC side of Mineirão's PV power plant, which were made at the point

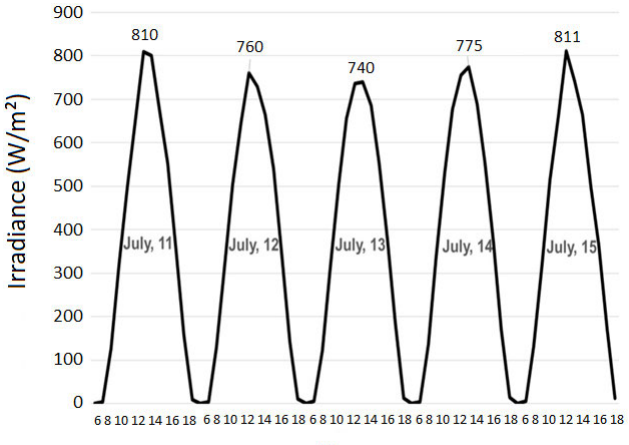

Days	Daily average Irradiation (kWh/m².day)
11/jul	4.87
12/jul	4.79
13/jul	4.89
14/jul	5.02
15/jul	4.09
Period mean	4.70

Days	Maximum irradiance (W/m²)
11/jul	810
12/jul	760
13/jul	740
14/jul	775
15/jul	811
Period mean	779

FIGURE 9. Global irradiance profile, by a horizontal pyranometer, for the measurement period.

of common coupling (PCC), and the global solar radiation, measured by an INMET horizontal pyranometer, were also monitored during the measurement campaign. These measurements are essential to understanding the behavior of the whole system during the period. Figure 9 illustrates the global irradiance during the five days.

As Figure 9 shows, the measurement campaign, which happened during sunny winter days and when clouds did not obscure the sky for the entire period, had an average of 4.70 kWh/m^2 for global daily average irradiation and 779 W/m^2 of mean maximum global irradiance.

To understand how the PV modules received incoming solar resource at each string influence according to their orientation (azimuth angles), Rüther *et al.* [29] selected eight sections (segments), of the 88 roof cover sections of Mineirão Stadium, with different orientations and the incoming solar radiation was estimated at the 8°-tilted plane. Figure 10 presents the annual average of the total daily global horizontal solar radiation and the radiation calculated at the 8°-tilted plane for the eight different azimuth angle deviations from true North, in kWh/m^2/day.

As Figure 10 shows, because the PV module array tilt is small (8°), the azimuth deviation of neighbor roof sections is small. It results in negligible differences in the resulting

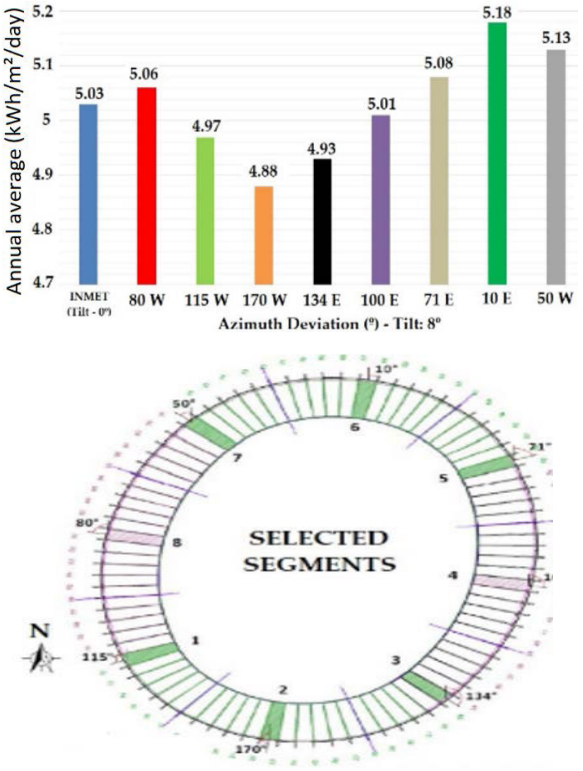

Figure Source adapted: [29]

	Segments							
	1	2	3	4	5	6	7	8
Annual Average (Absolute Relative Difference) - %	0.60	1.19	2.98	1.99	0.40	0.99	2.98	1.99
Absolute Relative Difference between Azimuth Deviation -%	1.78	1.81	1.02	1.62	1.40	1.97	0.97	1.38

FIGURE 10. The annual average of the total daily global horizontal solar radiation and the radiation calculated at the 8°-tilted plane for the eight different azimuth angle deviations from true North.

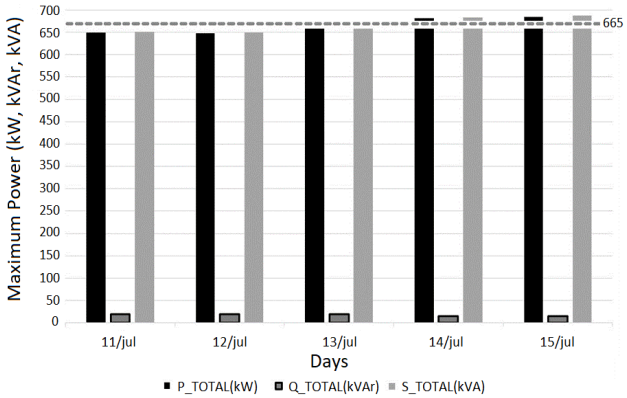

FIGURE 11. Maximum power generated for the monitored period.

incoming solar global irradiation availability between neighbor roof sections, i.e., annual average radiation relative difference ($\beta = 8°/\beta = 0°$), in general, is lower than 3% (e.g., segment 7) and between azimuth deviation, the absolute relative difference is less than 2% overall.

Figure 11 illustrates the maximum power results for the period.

TABLE 9. Electrical characteristics at STC for PV modules MPrime (data of the label in the posterior part of the PV module) and Tpsm (data obtained by a solar simulator describe before).

	PV Modules	
Electrical Parameters	**Mprime**	**Tpsm 2221**
V_{oc} (V)	37.6	21.6
I_{sc} (A)	8.60	1.47
V_{mpp} (V)	29.60	17.66
I_{mpp} (A)	8.24	1.31
P_{mpp} (W)	243.81	22.17
Sorting range	0/+5 W	N/A
Measure tolerance	3%	N/A

With the available solar resource, presented in Figure 9, the PV system reached, on average, a maximum of 665 kW of active power (grey dash bar in Figure 11). This value, when reflected from the DC side, considering a 98.5% DC–AC conversion efficiency of all Ingeteam 15 TL inverters plus transformers efficiency of 97%, is estimated as being approximately equal to 695 kW, i.e., 49% of the PV system's installed power (1.42 MWp).

It is essential to consider that the rated installed power is given at the STC, and as shown in Figure 9, the average maximum daily irradiance during the monitored period was far from such standard reference, which partially explains the reduced power output. Furthermore, other factors such as dust and soiling, partial shading of the PV generator, and the PV module's degradation contribute to the installation's performance reduction. Such factors are discussed in detail in the following subsections.

B. ACTUAL POWER AND I-V CURVES OF STRINGS PV1 AND PV2 GENERATORS

This section shows and discusses the results of actual power and I-V curve measurements at the strings of the PV1 and PV2 generators. First, it presents the measurements taken in one PV module randomly chosen from a PV generator at segment 13. After that, the results of measurements performed in all segments, as shown in Table 1, are presented.

1) MEASUREMENTS IN ONE PV MODULE

The measurements were made using the previously described capacitive loads and, initially, with the PV module in present conditions, i.e., with soiling and dust. After that, the PV module was cleaned, and measurements were then performed for this condition. Table 9 illustrates the electrical characteristics at standard test conditions (STC) for PV modules: MPrime—M 240 P model (data are taken from the label in the posterior part of the PV module), and model Tpsm 222155E (reference PV module—data obtained using a solar simulator, as previously described). Figures 12a,b, and 13a,b shows the results obtained by the measurements at these two distinct situations (soiling/clean).

Figures 12a,b, and 13a,b illustrates the MPrime and reference PV modules' results. These results show, for each measurement, the following variables: global irradiance (G), cell temperature of the device under test (DUT), i.e., MPrime PV module ($T_{c,DUT}$), cell temperature of the reference PV module ($T_{c,REFMOD}$), power measured at reference ($P_{measured\_REF}$) and MPrime ($P_{measured\_Soiling}$ and $P_{measured\_Clean}$) PV modules, power extrapolated to STC for reference ($P_{extra,STC\ REF}$) and MPrime ($P_{extra,STC}$) PV Modules. Moreover, the results also show the relative differences between $P_{extra\ STC}$ (for reference and MPrime PV modules), the power data 22.17 W (obtained by a solar simulator, see Table 9), and 243.81 W (from the label in the posterior part of the MPrime PV module, see Table 9).

As shown in Figure 12b, under soiling conditions, the average power measured using the two capacitive loads used is close (110.93 W GEDAE and 115.23 W Solmetric) for similar irradiance and cell temperature conditions: a relative difference of 3.7% was verified. When these measurements were extrapolated to STC, the relative difference decreased to 2.4%. Therefore, this difference shows consistency between the measurements made by GEDAE and Solmetric capacitive loads. Figure 12a shows good consistency between the measurements made in the PV reference module for both loads used. Results show a relative average difference concerning the reference PV module in Table 9: 1.94% (GEDAE) and 2.2% (Solmetric).

The mean error obtained from the reference PV module can be used to correct the STC power obtained for the DUT, i.e., 179.96 W+1.94% (183.45 W uses GEDAE load) and 184.45 W + 2.2% (188.51 W with Solmetric load). Therefore, the error parameter found demonstrates the reliability of using this PV module as a reference for all measurements. Finally, the results for the relative difference for the MPrime PV module (DUT Table 9), on average, were high (−26.19% GEDAE load and −24.35% Solmetric load).

When the MPrime PV module was cleaned, Figure 13b, under clean conditions, the average power measured by the two capacitive loads approaches (126.17 W GEDAE load and 126.88 W Solmetric load) for similar irradiance and cell temperature conditions. The relative difference is smaller than 1.0%. When these measurements are put in STC, a 1.6% relative difference is observed. Figure 13a still shows a good relationship for reference PV module with an error parameter (relative difference) of about 3.25% (GEDAE) and 3.20% (Solmetric) on average.

Comparing the relative difference for the DUT, the results get lower on average, compared to results from Figure 12a,b, but are still high for a PV module without soiling and dust (−17.91% GEDAE load and −19.22% SOLMETRIC load). Therefore, a decisive contribution, for power reduction, of about 8.28% (GEDAE load) and 5.13% (Solmetric load)—6.7% on average—was found for the soiled/clean PV module, respectively. Figures 14 and 15 show examples of I-V and P-V curves measured for the DUT—MPrime PV soiled/clean module.

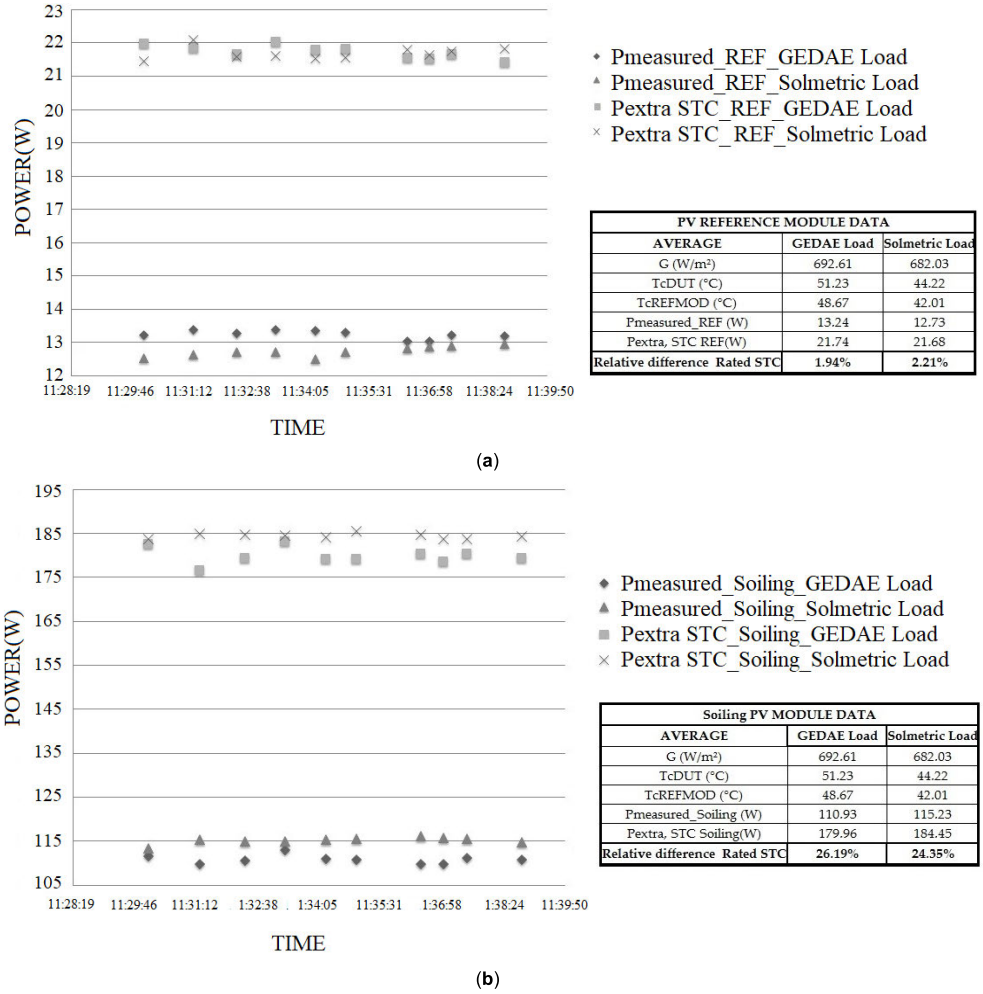

PV REFERENCE MODULE DATA		
AVERAGE	GEDAE Load	Solmetric Load
G (W/m²)	692.61	682.03
TcDUT (°C)	51.23	44.22
TcREFMOD (°C)	48.67	42.01
Pmeasured_REF (W)	13.24	12.73
Pextra, STC REF(W)	21.74	21.68
Relative difference Rated STC	**1.94%**	**2.21%**

Soiling PV MODULE DATA		
AVERAGE	GEDAE Load	Solmetric Load
G (W/m²)	692.61	682.03
TcDUT (°C)	51.23	44.22
TcREFMOD (°C)	48.67	42.01
Pmeasured_Soiling (W)	110.93	115.23
Pextra, STC Soiling(W)	179.96	184.45
Relative difference Rated STC	**26.19%**	**24.35%**

FIGURE 12. **(a) Measurements with capacitive loads (GEDAE/Solmetric) under soiling conditions (a) in reference PV module; (b) DUT MPrime PV module.**

As shown in Figures 14 and 15, it is clear the difference between the I-V curves and the power obtained for a PV module with soiling and dust and with a clean PV module cleaned. The STC extrapolated power loss contribution value found for soiling and dust was 10% from these measurements.

2) MEASUREMENTS AT STRINGS PV1 AND PV2 GENERATORS

In the same way that the measurements were performed in one PV module (DUT—MPrime—M 240 P model), they were performed on the strings of the PV1 and PV2 generators at segments shown in Table 1 and Figure 5. The measurements were performed by the two capacitive loads and the reference PV module, as illustrated in Table 10a,b.

It is essential to point out that all the strings of PV1 and PV2 were with soiling and dust. Furthermore, the results presented in Table 10a,b are a summary showing the average values found in the measurements for all segments considered in this study. It is possible to see in Table 10a,b, where all measurements are set approximately at the same conditions for G and T_c ($P_{extra\ STC}$), the influence of all segments' orientation on the final results. Segments 55, 64, and 67, which are oriented to the geographic north (see Figure 5), have the highest measured power achieved during the measurement campaign (e.g., 1,945 Wp—PV1/21.64 Wp—reference PV module; 1,965 Wp—PV2/21.74 Wp—reference PV module for segment 67 with GEDAE load). It is important to remember that, although the measurements were made during winter for the southern hemisphere, the sun is entire to the north of Belo Horizonte city. Therefore, this region of the Mineirão PV power plant is expected to perform better than other regions.

In the south region (segments 11 to 33), PV1 and PV2 generators from segment 13 achieved the lowest power values, as expected (e.g., 1,635 Wp—PV1/20.25 Wp—reference module; 1,641 Wp—PV2/20.50 Wp—reference module with GEDAE load). The relative power difference is about 16% compared to PV1 and PV2 generators in segment 67. This value could be reduced to approximately 11% when associating with the relative power difference obtained from the

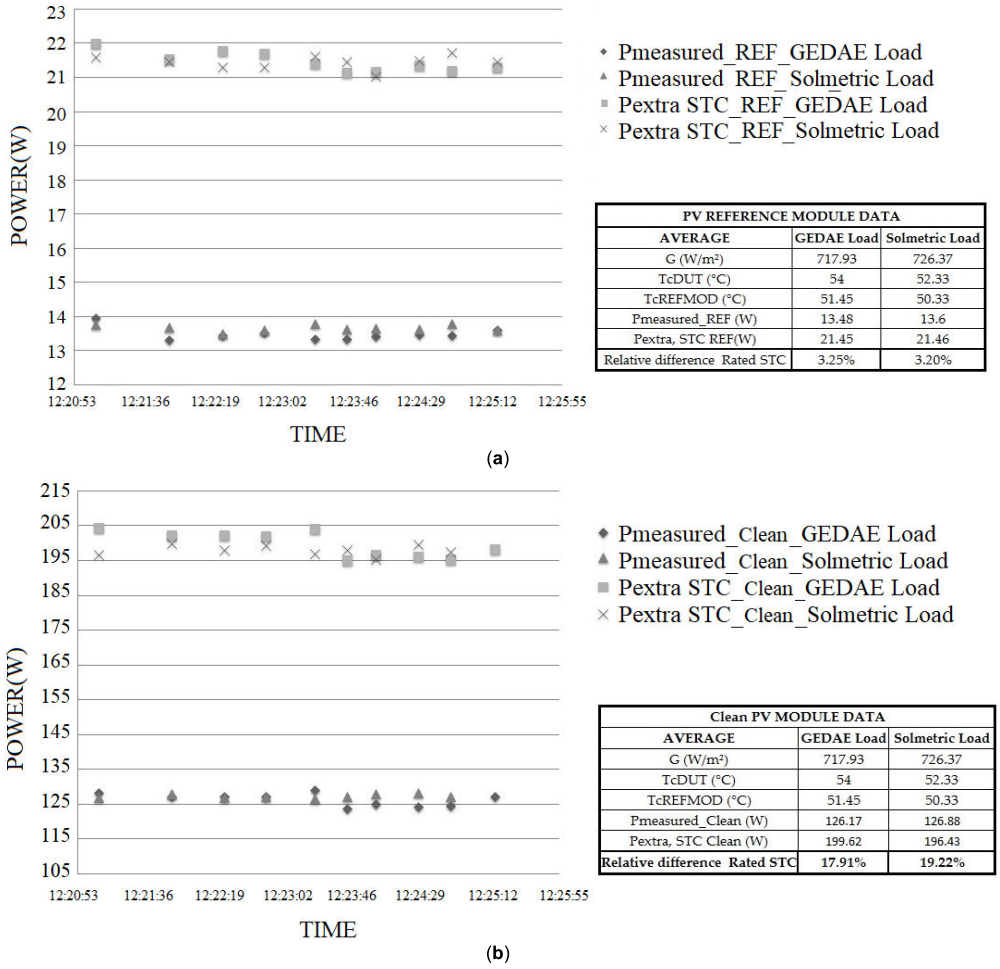

PV REFERENCE MODULE DATA		
AVERAGE	GEDAE Load	Solmetric Load
G (W/m²)	717.93	726.37
TcDUT (°C)	54	52.33
TcREFMOD (°C)	51.45	50.33
Pmeasured_REF (W)	13.48	13.6
Pextra, STC REF(W)	21.45	21.46
Relative difference Rated STC	3.25%	3.20%

Clean PV MODULE DATA		
AVERAGE	GEDAE Load	Solmetric Load
G (W/m²)	717.93	726.37
TcDUT (°C)	54	52.33
TcREFMOD (°C)	51.45	50.33
Pmeasured_Clean (W)	126.17	126.88
Pextra, STC Clean (W)	199.62	196.43
Relative difference Rated STC	17.91%	19.22%

FIGURE 13. (a) Measurements with capacitive loads (GEDAE/Solmetric) under clean conditions (a) in reference PV module; (b) DUT MPrime PV module.

reference PV module, in each measure, at the corresponding PV generator.

For generators PV1 and PV2 located at segments 37 and 45 (east region—segments 34 to 54), the performance was better (4% higher on average) compared to the generator PV1 (segment 01) at the west region (segments 10 to 78) as Table 10a,b shows. This fact probably occurred because the measurements were taken during the morning for east generators. Therefore, this side was favored.

Except for the south region of Mineirão Stadium, all the measurement results presented in Table 10a show an excellent approach to the reference PV module parameters presented in Table 9. This result indicates the good performance of the used methodology, even when irradiance levels are outside the recommended range of 800 to 1,100 W/m^2, with an absolute difference lower than 4%, and with an average difference value of −2.9%.

To further investigate the influence of the STC extrapolation methodology on the results, PV1 and PV2 generator measurements for all measured regions were extrapolated to photovoltaics for utility-scale applications test conditions (PTC) (1,000 W/m^2, 20 °C air temperature, and wind speed of 1 m/s at 10 m above ground level, air mass 1.5). These results represent an operating condition closer to the actual PV generator field operation, given at a PV cell temperature of 45 °C. The PTC ratings for the Mprime module are not available in its datasheet; however, it was possible to obtain an approximate value of its PTC-rated power from the I-V curve given in the datasheet, taken at a cell temperature of 45 °C, which is: $P_{rated,PTC} = 210.40$ W. Table 11 summarizes the PTC extrapolation results. It is possible to observe that when compared to PTC conditions, the extrapolated data has a reduction in the relative difference from rating values; however, this difference is still considerable, i.e., −15.64% (total mean).

Comparing the measurement regions (north, east, and west) for the strings with Mprime PV modules with DUT, the results were also high, with an absolute average of 22%, as in the measurements performed with two loads in one PV module (26.19% GEDAE and 24.35% Solmetric, Figure 12a,b).

Considering an average power reduction due to soiling and dust of about 6.7% (already found in this study), and

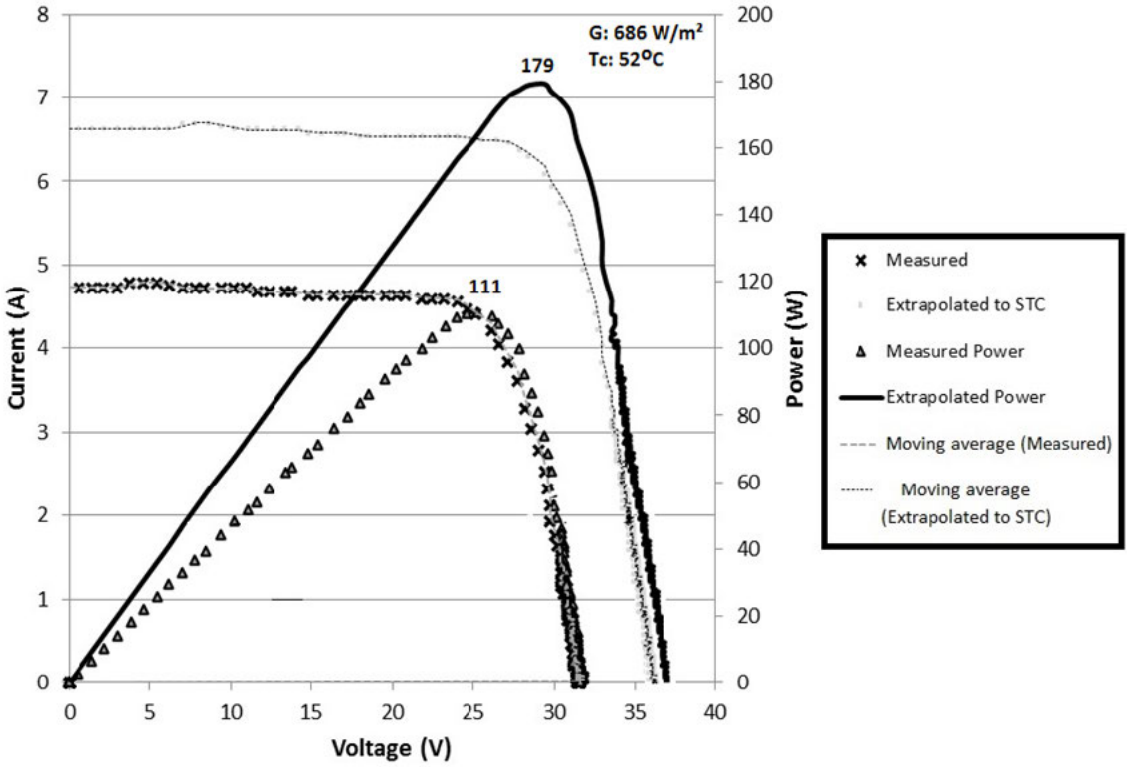

FIGURE 14. Sample of I-V/power curves obtained for the MPrime PV module with soiling and dust.

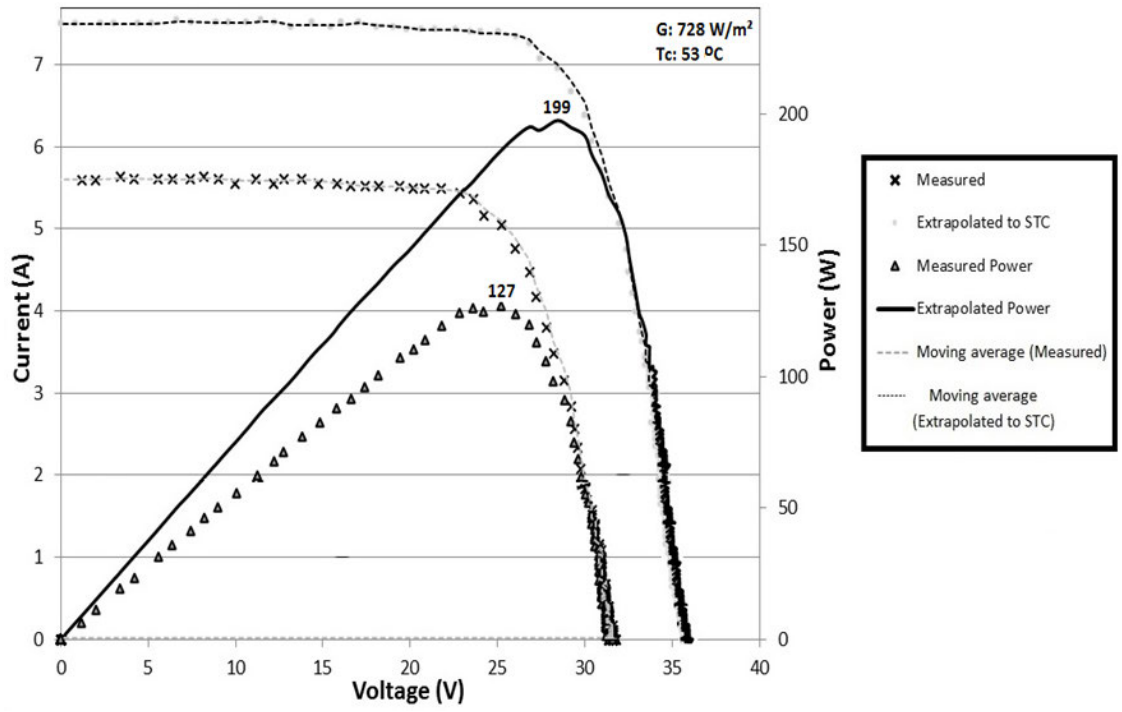

FIGURE 15. Sample of I-V/power curves obtained for the MPrime PV module after being cleaned.

associating the average measurement error in the reference PV module of −2.9% to the PV generators, the absolute average difference value for PV generators decreases from 22% to 12.4%. The last value corresponds to the percentage

TABLE 10. Measurements in (A) the reference PV module and (B) strings of PV1 and PV2 generators at segments with capacitive loads.

	(a) Information					Reference PV Module		Relative Difference
Regions	Segment/Date/Load/Generator	Hour	G(W/m^2)	T_{cDUT}(°C)	$T_{cREFMOD}$ (°C)	$P_{measured}$ (W)	$P_{extra\ STC}$ (W)	Reference Mod. Table 9
North	67/11 Jul/Gedae/PV2	11:33–11:47 a.m.	810.23	55.99	53.19	14.91	21.74	−1.94%
	67/11 Jul/Gedae/PV1	11:06–11:29 a.m.	799.71	56.94	54.09	14.87	21.64	−2.39%
	64/15 Jul/Gedae/PV1	10:54–11:11 a.m.	812.87	54.88	52.14	14.92	21.75	−1.89%
	64/15 Jul/Solmetric/PV1	11:31–11:34 a.m.	809.23	51.89	49.29	14.90	21.68	−2.21%
	55/12 Jul/Gedae/PV1	12:00–12:10 p.m.	766.72	51.85	49.26	14.42	21.60	−2.57%
	55/12 Jul/Gedae/PV2	12:12–12:16 p.m.	755.78	50.84	48.30	14.24	21.40	−3.47%
East	45/12 Jul/Gedae/PV2	10:43–10:50 a.m.	809.14	53.93	51.23	14.41	21.45	−3.25%
	37/14 Jul/Gedae/PV1	10:41–10:57 a.m.	738.47	45.82	43.53	14.38	21.44	−3.29%
	37/14 Jul/Solmetric/PV1	11:18–11:25 a.m.	705.56	43.17	41.01	14.40	21.45	−3.27%
	45/12 Jul/Gedae/PV1	10:36–10:42 a.m.	753.27	53.65	50.97	14.30	21.44	−3.28%
West	01/14 Jul/Gedae/PV1	12:31–12:52 p.m.	763.30	53.29	50.63	14.37	21.30	−3.92%
	01/14 Jul/Solmetric/PV1	12:59–13:05 p.m.	747.01	49.28	46.81	14.36	21.44	−3.29%
South	13/13 Jul/Solmetric/PV1	10:29–10:43 a.m.	618.45	39.58	37.60	12.14	20.00	−9.79%
	13/13 Jul/Gedae/PV2	10:48–10:56 a.m.	655.34	48.29	45.88	12.73	20.50	−7.53%
	13/13 Jul/Gedae/PV1	10:29–10:43 a.m.	621.13	46.82	44.48	12.44	20.25	−8.66%
		Total Mean	**744.41**	**50.42**	**47.89**	**14.12**	**21.27**	**−4.05%**
	(b) Information					**PV1 and PV2**		**Relative Difference**
Regions	**Segment/Date/Load/Generator**	**Hour**	**G(W/m^2)**	**T_{cDUT}(°C)**	**$T_{cREFMOD}$ (°C)**	**$P_{measured}$ (W)**	**$P_{extra\ STC}$ (W)**	**DUT Table 9**
North	67/11 Jul/Gedae/PV2	11:33–11:47 a.m.	810.23	55.99	53.19	1,397	1,965	−19.40%
	67/11 Jul/Gedae/PV1	11:06–11:29 a.m.	799.71	56.94	54.09	1,388	1,945	−20.22%
	64/15 Jul/Gedae/PV1	10:54–11:11 a.m.	812.87	54.88	52.14	1,365	1,921	−21.21%
	64/15 Jul/Solmetric/PV1	11:31–11:34 a.m.	809.23	51.89	49.29	1,362	1,892	−22.40%
	55/12 Jul/Gedae/PV1	12:00–12:10 p.m.	766.72	51.85	49.26	1,278	1,885	−22.69%
	55/12 Jul/Gedae/PV2	12:12–12:16 p.m.	755.78	50.84	48.30	1,265	1,853	−24.00%
East	45/12 Jul/Gedae/PV2	10:43–10:50 a.m.	809.14	53.93	51.23	1,156	1,735	−20.93%
	37/14 Jul/Gedae/PV1	10:41–10:57 a.m.	738.47	45.82	43.53	1,141	1,715	−21.84%
	37/14 Jul/Solmetric/PV1	11:18–11:25 a.m.	705.56	43.17	41.01	1,141	1,741	−20.66%
	45/12 Jul/Gedae/PV1	10:36–10:42 a.m.	753.27	53.65	50.97	1,119	1,715	−21.84%
West	01/14 Jul/Gedae/PV1	12:31–12:52 p.m.	763.30	53.29	50.63	1,115	1,667	−24.03%
	01/14 Jul/Solmetric/PV1	12:59–13:05 p.m.	747.01	49.28	46.81	1,116	1,653	−24.67%
South	13/13 Jul/Solmetric/PV1	10:29–10:43 a.m.	618.45	39.58	37.60	1,105	1,652	−32.24%
	13/13 Jul/Gedae/PV2	10:48–10:56 a.m.	655.34	48.29	45.88	1,100	1,641	−32.69%
	13/13 Jul/Gedae/PV1	10:29–10:43 a.m.	621.13	46.82	44.48	1,057	1,635	−32.94%
		Total Mean	**744.41**	**50.42**	**47.89**	**1,215**	**1,774**	**−24.12%**

TABLE 11. PV1 and PV2 generator's measurement and extrapolation to photovoltaics for utility-scale applications test conditions (PTC) for the north, east, and west regions.

Region	Segment/Date/Load/ Generator	$P_{measured}$ (W)	$P_{extra,PTC}$ (W)	Relative Difference from DUT (Table 9) at $P_{rated,PTC}$
North	67/11 Jul/Gedae/PV2	1,388	1,810	−13.92%
	67/11 Jul/Gedae/PV1	1,397	1,833	−12.83%
	64/15 Jul/Gedae/PV1	1,365	1,757	−16.47%
	64/15 Jul/Solmetric/PV1	1,362	1,761	−16.25%
	55/12 Jul/Gedae/PV1	1,278	1,719	−18.29%
	55/12 Jul/Gedae/PV2	1,265	1,752	−16.70%
East	45/12 Jul/Gedae/PV2	1,156	1,513	−20.11%
	37/14 Jul/Gedae/PV1	1,141	1,596	−15.72%
	37/14 Jul/Solmetric/PV1	1,141	1,620	−14.45%
	45/12 Jul/Gedae/PV1	1,119	1,557	−17.79%
West	01/14 Jul/Gedae/PV1	1,115	1,501	−20.74%
	01/14 Jul/Solmetric/PV1	1,116	1,538	−18.76%
South	13/13 Jul/Solmetric/PV1	1,105	1,912	−9.11%
	13/13 Jul/Gedae/PV2	1,100	1,841	−12.46%
	13/13 Jul/Gedae/PV1	1,057	1,872	−10.99%
	Total Mean:	**1,207**	**1,705**	**−15.64%**

in which real installed power is less than the nominal power, which implies a real peak power of 1.24 MWp (1.42 MWp−12.4%). Applying the uncertainty found in this study, 4.6% for power in STC, and considering the value of 1.24 MWp for the whole plant, the real peak power could be between 1.183 MWp and 1.297 MWp.

The considerable difference between real-power and rated-power values influences Mineirão's PV power plant's whole performance analyses. It is worth mentioning that the PVSyst simulations for the solar plant presented a mean daily energy production of 4.4 MWh, according to the Martifier Solar report [31]. The corresponding final yield of 3.1 kWh/kWp was obtained, considering the rated power of 1.42 MWp.

The study presented in [22] analyzed the performance ratio (PR) for the Mineirão Stadium PV plant for over a year of measured data. The monthly PR results calculated from nameplate data for installed PV power (1.42 MWp) are represented in the light gray bars of Figure 16. Updated PR calculations that consider measured installed PV power (1.24 MWp) are represented by the dark gray bars. Figure 16 illustrates that PR's smallest values, happening in months with fewer solar radiation, consequently low PV productivity, while higher values are reached in sunnier months. To estimate this parameter, this research uses the global irradiation data from the INMET meteorological station, described in the previous section, and the PR equation, as defined in [51]. It is possible to notice that the system's PR varies between 0.82 and 0.71 over the year, presenting an annual average of 0.76 (black dashed line) between 2014 and 2015. It can be seen that the correct PR value (evaluated for measured, installed PV power) is higher than the value obtained from datasheet values, highlighting the importance of such commissioning for the correct evaluation of the performance of a system. Table 12 shows the summary of different situations (scenarios) according to the installed capacity considered.

The PR variation over the year (0.82 to 0.71) is mainly explained by the shadowing that occurs differently as the seasons change. [22] shows an evaluation of shadowing at the segments of the Mineirão PV plant using the PVSyst

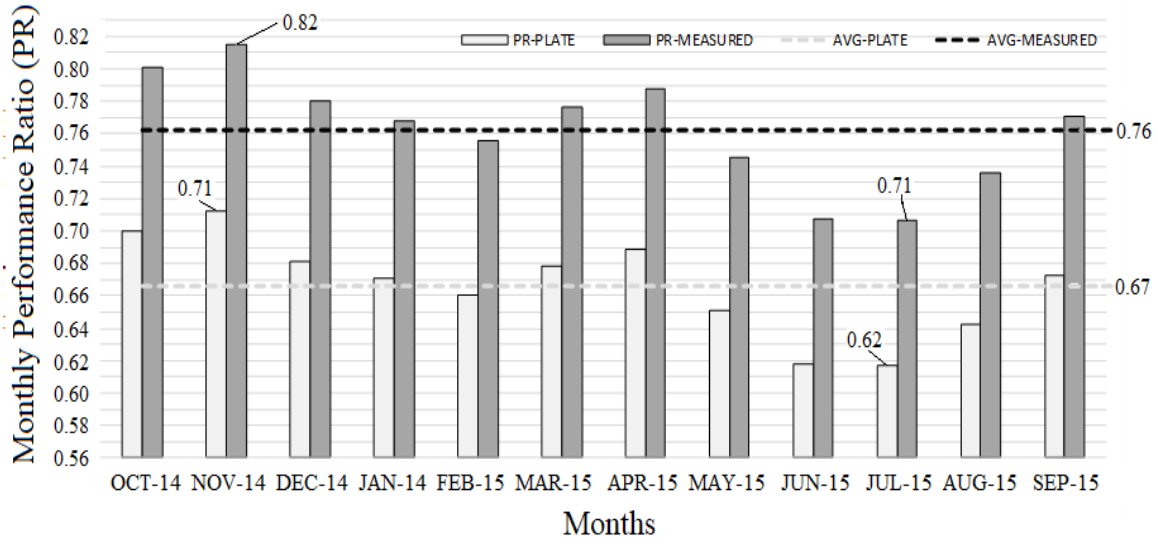

FIGURE 16. PV system performance ratio for both nameplate and measured PV installed capacity. PR: Performance Ratio.

TABLE 12. Summary of final yields and PR for monitoring data and PVSyst simulation calculated based on datasheet PV power information and measured PV power information.

Type of data		Monitoring	PVSyst	Relative Difference (%)
Energy Production (MWh/year)		1,761	1,610	9.38
Annual Yf (kWh/kWp); PR(%)	Pn(kW)=1.42	1,240; 66	1,134; 72	9.34; 8.33
	Pn(kW)=1.24	1,420; 76	1,298; 82	9.40;-7.32
	Pn(kW)=1.183	1,488; 80	1,360; 86	9.41;-6.98
	Pn(kW)=1.297	1,357; 73	1,241; 79	9.35;-7.59
Reference Irradiation (kWh/m^2.day^{-1})		5.18	4.32	16.6

software. Figure 17a, b shows the simulation results obtained in [22] for segment 67 (facing north). From the shading diagram presented in Figure 17b, it is possible to see that shading loss is larger during the winter season (from May to August), while in the summer season, shading is less intense. Under no shading conditions, the PR of a system tends to have higher values during winter, the dominant factor being the operating temperature.

For the Mineirão's PV power plant, in general, shadows are typical in the morning (beginning around 8:00 a.m., with 40% shading loss, and ending about 9:30 a.m., with 1% shading loss) and late in the afternoon (beginning approximately 3:00 p.m., with 5% shading loss, and ending about 4:00 p.m., with 40% shading loss) during the year.

In 2019, a shading study considering the 3D model of Mineirão stadium was published [57]. This article's results show 4.3% for annual effective shading losses in the entire PV power plant. The most affected areas are north and south, with 5.6%, while the lower value is 2.2% in the west and east areas. The model [58] used to calculate PV system losses is based on geometric shading and the number of active by-pass diodes to simplify the simulation. Shading cases are often discussed at distortions shown in I-V curves. As an example, [59] describe the shading effect in multiple maximum power points, [60] show curve patterns in horizontal and vertical module shading, and [61] compare types of string connections to maximize power in shading situations.

Another Mineirão's PV shading study was conducted by Rüther *et al.* [29]. The research was performed on the roof cover sections of the Mineirão stadium and consisted of selected eight individual segments, see Figure 10, representing the 88 individual sections of the Mineirão roof cover for a detailed analysis of the shading effects using Ecotect software. Table 13 shows the consolidated shading analysis, with the resulting solar radiation incident on each segment with and without shading.

As Table 13 presents, with shading, a 15.19% annual average incident solar radiation of reduction was found on the PV segments of Minerão stadium.

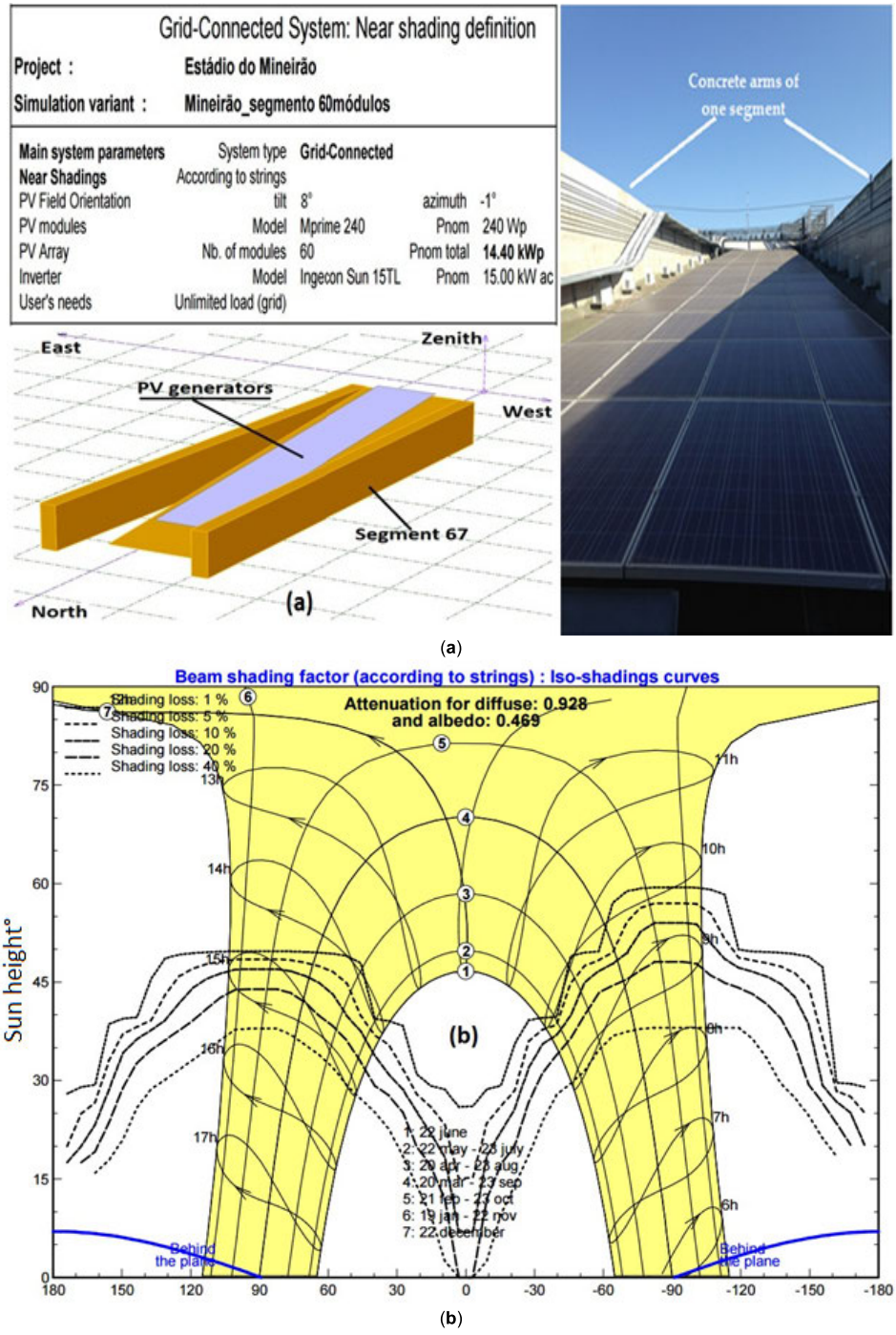

FIGURE 17. (a) Data input/3D drawing in PVsyst software and photo presenting shading early in the morning; and (b) shading diagram for this segment [22].

Considering Pvsyst simulation [22] the annual energy production of 1,761 MWh and the obtained PV power of 1.24 MWp, an average daily yield of 3.89 kWh/kWp is found. Therefore, the system presented a good final daily yield during the period, if compared to other PV systems installed, for example, in Germany, Italy, the USA, and Australia, where the average final yield varies from 2.54 ± 0.24 kWh/kWp to 5.22 ± 0.44 kWh/kWp, IEA [52]. In the metropolitan area of Belo Horizonte, the same region where the system is installed, the final daily yield varies from 3.68 ± 0.51 kWh/kWp to 4.01 ± 0.64 kWh/kWp (Nolasco *et al.*, [53]) and, also, from the simulation of the Mineirão PV system in PVsyst software [44], a value of 3.21 kWh/kWp was found.

Finally, it is well-known in the literature [33], [54], [55] that the rates of c-Si PV degradation of power, on average, range from about 0.70% to 0.90% per year. The PV modules

TABLE 13. Monthly means of the daily average incident solar radiation (kWh/m^2/day) on each segment, with and without shading.

WITHOUT SHADING											
Segment			*1*	*2*	*3*	*4*	*5*	*6*	*7*	*8*	
Tilt angle			8°	8°	8°	8°	8°	8°	8°	8°	
Azimuth Deviation			80° W	115° W	170° W	134° L	100° L	71° L	10° L	50° W	
Irradiation		Horizontal									
kWh/m²/day	JAN	5.90	5.90	5.93	5.95	5.94	5.91	5.89	5.86	5.87	
	FEB	6.20	6.20	6.19	6.18	6.18	6.20	6.21	6.23	6.22	
	MAR	5.60	5.63	5.55	5.48	5.52	5.59	5.65	5.73	5.69	
	APR	5.50	5.55	5.36	5.17	5.27	5.44	5.60	5.80	5.69	
	MAY	4.20	4.23	4.06	3.90	3.98	4.13	4.27	4.47	4.37	
	JUN	4.30	4.35	4.09	3.85	3.97	4.20	4.42	4.70	4.55	
	JUL	4.30	4.34	4.11	3.90	4.01	4.20	4.40	4.65	4.52	
	AUG	4.40	4.44	4.30	4.16	4.23	4.36	4.48	4.63	4.55	
	SEP	4.90	4.94	4.85	4.77	4.81	4.89	4.96	5.05	5.00	
	OCT	5.60	5.62	5.58	5.55	5.57	5.60	5.63	5.67	5.65	
	NOV	4.80	4.81	4.82	4.83	4.82	4.82	4.81	4.80	4.81	
	DEC	4.70	4.72	4.74	4.75	4.74	4.73	4.71	4.69	4.71	
Annual Average		5.03	5.06	4.97	4.87	4.92	5.01	5.09	5.19	5.14	
WITH SHADING											
Segment			1	2	3	4	5	6	7	8	
Tilt angle			8°	8°	8°	8°	8°	8°	8°	8°	
Azimuth Deviation			80° W	115° W	170° W	134° L	100° L	71° L	10° L	50° W	Monthly Average	Reduction Average
Irradiation		Horizontal										
kWh/m²/day	JAN	5.90	4.86	5.36	4.83	5.31	5.87	5.62	4.96	5.25	5.26	10.89%
	FEB	6.20	5.11	5.81	4.99	5.53	6.19	5.83	5.24	5.66	5.54	10.61%
	MAR	5.60	4.51	5.26	4.36	4.69	5.28	5.08	4.67	5.09	4.87	13.12%
	APR	5.50	4.51	5.04	4.16	4.39	3.71	4.63	4.80	5.02	4.53	17.55%
	MAY	4.20	3.47	3.48	3.17	3.14	2.26	3.02	3.67	3.70	3.24	22.87%
	JUN	4.30	3.51	3.44	3.03	3.07	2.28	2.60	3.95	3.87	3.22	25.16%
	JUL	4.30	3.59	3.54	3.05	3.12	2.29	2.89	4.00	3.86	3.29	23.42%
	AUG	4.40	3.63	3.89	3.30	3.45	2.54	3.45	3.83	3.93	3.50	20.40%
	SEP	4.90	3.99	4.65	3.99	4.02	4.23	4.32	4.20	4.50	4.24	13.56%
	OCT	5.60	4.57	5.32	4.65	4.84	5.58	5.32	4,81	5.15	5.03	10.20%
	NOV	4.80	3.92	4.51	4.01	4.29	4.75	4.62	3.93	4.32	4.29	10.55%
	DEC	4.70	3.93	4.33	3.93	4.17	4.65	4.53	3.93	4.25	4.21	10.34%
Annual Average		5.03	4.13	4.55	3.96	4.17	4.14	4.33	4.33	4.55	4.27	15.19%
Percentage reduction			18.35%	8.34%	18.83%	15.31%	17.36%	14.94%	16.52%	11.40%		

Source: adapted from [29].

of the Mineirão Stadium were installed from 2012 to 2013, and the PV power plant was commissioned in December 2013. Thus, the plant has been in official operation for three years up to the measurement campaign's date. Theoretically, it should have presented a total power degradation of about 2.10% (for a conservative degradation rate of 0.70%/year). This number is six times lower than the one obtained before (−12.4%).

V. CONCLUSION

This work presented the results of five days of on-site I-V curve measurements in several sub generators of a 1.42 MWp PV power plant installed at Mineirão Football Stadium's rooftop in the city of Belo Horizonte city, Brazil. The results made it possible for engineers and researchers to obtain the real peak power and the uncertainty associated with the measurement process—values rarely found in the analyses of the

performance of the big PV power plants installed at stadiums worldwide.

The results were found by performing measurements with commercial (Solmetric) and a self-made capacitive load (GEDAE), with a difference between the two systems of less than 2.4%. The self-made GEDAE capacitive load is a significant advance for the measurement of parameters, with robust results compared to the Solmetric capacitive load, even at the same time (operating conditions) of the DUT. A reference PV module was used to reduce the absolute average measurement error. The reference PV module was previously tested in an "A + A + A +" solar simulator, which rendered the nominal parameters exceptionally reliable.

Comparing the measurement values extrapolated to STC with power data from the label in the posterior part of one MPrime PV module, it was possible to estimate the impact of soiling and dust in the power reduction at the PV power plant to be about 6.7%.

As with the measurements performed in one PV module, measurements were also carried out in strings of PV1/PV2 generators at segments with both capacitive loads and a reference PV module. First, the influence of segment orientation and the time at which the measurement was performed was evident for segments in the east, west, and north areas since they present the lowest relative difference percentage in terms of power generation.

Regarding the measured values extrapolated to STC, when compared to the power data from labels of the MPrime PV module (considering the whole string), in absolute average, the results were still high, 22%, as occurred in the measurements performed with both capacitive loads in one PV module.

Considering that all PV modules from PV1/PV2 generators were cleaned (so without dust—6.7%) and disregarding the absolute average associated error of 2.9% that was found, the relative value goes down to 12.4%. This value is six-times-higher than the typical value of degradation for three years of operation (2.1%).

The final real peak power obtained was 12.4% lower than the one obtained by the sum of the individual rated power of the PV modules, resulting in a 1.24 MWp of installed capacity of the plant (1.42 MWp—12.4%). Applying the uncertainty found in this study, 4.6% for power in STC, and considering the value presented before for the whole plant, the real peak power could be between 1.183 MWp and 1.297 MWp.

A low final average daily final yield for the five days of measurements was found. Therefore, three hypotheses may be proposed based on this situation and could explain such poor performance: first, shadowing over the panels during the day caused by the concrete arms of each segment is constant over the year; second, the contribution of soiling and dust may contribute to this low value; and third, the actual peak power of the mounted PV modules is significantly lower than their rated power.

This experience brings essential results about PV power plants' quality assurance and describes a methodology that can be performed to determine the actual peak power without expensive solar simulators. This methodology could be applied in many developing countries, introducing PV power plants into their electrical system. Cases where the actual parameters differ significantly from those made available in the datasheets, can harm the investor, who may overestimate the initial cost. Consequently, the monetary return will not occur at the expected time. Ensuring system quality through testing and verifications from design and planning to execution and operation avoids this problem.

Finally, taking advantage of the fact that UFV-Mineirão is installed in an urban area, another P and D Project, D0722, will evaluate its influence in urban feeders. Specifically, the UFV-Mineirão connection feeder is equipped with two battery energy storage systems (BESS). Such evaluation will provide a broad view of the interaction of medium voltage feeders, PV plants, and energy storage systems. These results are to be published soon.

ACKNOWLEDGMENT

The authors appreciate the National Institute of Meteorology (INMET), Group of Studies, and Development of Alternatives Energy (GEDAE) from the Federal University of Pará (UFPA), and the Electrical Engineering Graduate Program (PPGEE) from the Universidade Federal de Minas Gerais (UFMG).

REFERENCES

[1] W. Herrmann, G. Belluardo, and B. Herteleer, "Photovoltaic module energy yield measurements: Existing approaches and best practice," Int. Energy Agency (IEA)-Photovoltaic Power Syst. Programme, Manno, Switzerland, Tech. Rep. IEA-PVPS T13-11:2018, 2018, p. 134.

[2] C. Reise, B. Müller, D. Moser, G. Belluardo, and P. Ingenhoven, "Uncertainties in PV system yield predictions and assessments," Int. Energy Agency (IEA)-Photovoltaic Power Syst. Programme, Manno, Switzerland, Tech. Rep. IEA-PVPS 915 T13-12:2018, 2018, p. 74.

[3] R. Srivastava, A. N. Tiwari, and V. K. Giri, "An overview on performance of PV plants commissioned at different places in the world," *Energy Sustain. Develop.*, vol. 54, pp. 51–59, Feb. 2020.

[4] I. D. L. Parra, M. Muñoz, E. Lorenzo, M. García, J. Marcos, and F. Martínez-Moreno, "PV performance modelling: A review in the light of quality assurance for large PV plants," *Renew. Sustain. Energy Rev.*, vol. 78, pp. 780–797, Oct. 2017, doi: 10.1016/j.rser.2017.04.080.

[5] F. Martinez-Moreno, E. Lorenzo, L. Navarte, R. Moretón, N. Tyutyundzhiev, and I. D. L. Parra, "Technical specifications and quality control procedures for reducing the uncertainty in PV installations: Results of the FP7 project PVCrops," in *Proc. 31th Eur. PV Sol. Energy Conf. Exhib.*, Hamburg, Germany, 2015, pp. 2225–2229, doi: 10.4229/EUPVSEC20152015-5BV.2.15.

[6] J. Coello, L. Pérez, F. Domínguez, and M. Navarrete, "On-site quality control of photovoltaic modules with the PV MOBILE LAB," *Energy Procedia*, vol. 57, pp. 89–98, 2014, doi: 10.1016/j.egypro.2014.10.012.

[7] S. Sarikh, M. Raoufi, A. Bennouna, A. Benlarabi, and B. Ikken, "Implementation of a plug and play I-V curve tracer dedicated to characterization and diagnosis of PV modules under real operating conditions," *Energy Convers. Manage.*, vol. 209, Apr. 2020, Art. no. 112613, doi: 10.1016/j.enconman.2020.112613.

[8] G. TamizhMani and A. Mikonowicz, "Module power rating requirements," Solar America Board Codes Standards/Policy Recommendation Rep., U.S. Dept. Energy, Washington, DC, USA, Tech. Rep. DE-FC36-07GO17034, Mar. 2011, pp. 1–13.

[9] *European Commission Joint Research (JRC)/Centre Institute for Energy. Guidelines for PV Power Measurement in Industry*, JRC Sci., Ispra, Italy, 2014, p. 80.

[10] D. Drnberger, J. Bartke, A. Steinhüser, K. Kiefer, and F. Neuberger, "Uncertainty of field I-V-cuve measurements in large scale PV-systems," in *Proc. 25th EU PVSEC*, 2010, pp. 4587–4594, doi: 10.4229/25thEUPVSEC2010-4BV.1.62.

[11] M. Cáceres, A. Firman, J. Montes-Romero, A. R. G. Mayans, L. H. Vera, E. F. Fernández, and J. D. L. C. Higueras, "Low-cost I–V tracer for PV modules under real operating conditions," *Energies*, vol. 13, no. 17, p. 4320, Aug. 2020, doi: 10.3390/en13174320.

[12] R. Moreton, E. Lorenzo, and J. A. Munoz, "500-kW PV generator I-V curve," *Prog. Photovolt. Res. Appl.*, vol. 22, no. 12, pp. 1280–1285, 2014, doi: 10.1002/pip.2401.

[13] F. Martinez-Moreno, E. Lorenzo, J. Munoz, and R. Moretón, "On the testing of large PV arrays," *Prog. Photovolt. Res. Appl.*, vol. 20, no. 1, pp. 100–105, 2012, doi: 10.1002/pip.1102.

[14] E. Duran, M. Piliougine, M. Sidrach-de-Cardona, J. Galan, and J. M. Andujar, "Different methods to obtain the I–V curve of PV modules: A review," in *Proc. 33rd IEEE Photovolatic Spec. Conf.*, May 2008, pp. 1–6, doi: 10.1109/PVSC.2008.4922578.

[15] F. Spertino, J. Ahmad, A. Ciocia, P. Di Leo, A. F. Murtaza, and M. Chiaberge, "Capacitor charging method for I–V curve tracer and MPPT in photovoltaic systems," *Sol. Energy*, vol. 119, pp. 461–473, Sep. 2015, doi: 10.1016/j.solener.2015.06.032.

[16] J. M. Carrillo, F. Martínez-Moreno, C. Lorenzo, and E. Lorenzo, "Uncertainties on the outdoor characterization of PV modules and the calibration of reference modules," *Sol. Energy*, vol. 155, pp. 880–892, Oct. 2017, doi: 10.1016/j.solener.2017.07.028.

[17] *Photovoltaic (PV) Module Performance Testing and Energy Rating-Part 1: IRRADIANCE and Temperature Performance Measurements and Power Rating*; IEC Standard 61853-1, 2011.

[18] H. Müllejans, W. Zaaiman, and R. Galleano, "Analysis and mitigation of measurement uncertainties in the traceability chain for the calibration of photovoltaic devices," *Meas. Sci. Technol.*, vol. 20, no. 7, 2009, Art. no. 075101.

[19] K. Paghasian and G. TamizhMani, "Photovoltaic module power rating per IEC 61853-1: A study under natural sunlight," in *Proc. 37th IEEE Photovoltaic Spec. Conf.*, Seattle, WA, USA, 2011, pp. 002322–002327, doi: 10.1109/PVSC.2011.6186418.

[20] F. C. Treble, "On-site measurement of the performance of crystalline silicon PV arrays. Renew," *Energy*, vol. 5, pp. 275–280, Aug. 1994, doi: 10.1016/0960-1481(94)90383-2.

[21] M. M. Fraga, B. L. D. O. Campos, T. B. D. Almeida, J. M. F. D. Fonseca, and V. D. F. C. Lins, "Analysis of the soiling effect on the performance of photovoltaic modules on a soccer stadium in minas gerais, Brazil," *Sol. Energy*, vol. 163, pp. 387–397, Mar. 2018, doi: 10.1016/j.solener.2018.02.025.

[22] L. Monteiro, W. Macedo, P. Torres, A. Piterman, M. Silva, G. Amaral, B. Lopes, J. Fraga, and W. Boaventura, "One-year monitoring PV power plant installed on rooftop of mineirao FIFA world cup/olympics football stadium," *Energies*, vol. 10, no. 2, p. 225, Feb. 2017, doi: 10.3390/en10020225.

[23] H. A. Pereira, R. Teodorescu, F. D. Freijedo, M. M. Silva, and V. F. Mendes, "Harmonic current prediction by impedance modeling of grid-tied inverters: A 1.4 MW PV plant case study," *Int. J. Electr. Power Energy Syst.*, vol. 93, pp. 30–38, Dec. 2017, doi: 10.1016/j.ijepes.2017.05.009.

[24] S. F. A. Shah, I. A. Khan, and H. A. Khan, "Performance evaluation of two similar 100 MW solar PV plants located in environmentally homogeneous conditions," *IEEE Access*, vol. 7, pp. 161697–161707, 2019, doi: 10.1109/ACCESS.2019.2951688.

[25] B. S. Kumar and K. Sudhakar, "Performance evaluation of 10 MW grid connected solar photovoltaic power plant in India," *Energy Rep.*, vol. 1, pp. 184–192, Nov. 2015, doi: 10.1016/j.egyr.2015.10.001.

[26] S. Sundaram and J. S. C. Babu, "Performance evaluation and validation of 5MWp grid connected solar photovoltaic plant in South India," *Energy Convers. Manage.*, vol. 100, pp. 429–439, Aug. 2015, doi: 10.1016/j.enconman.2015.04.069.

[27] J. Muñoz, E. Lorenzo, J. M. Carrillo, and R. Moretón, "Design of a twin capacitive load and its application to the outdoor rating of photovoltaic modules," *Prog. Photovolt., Res. Appl.*, vol. 23, no. 2, pp. 247–252, Feb. 2015, doi: 10.1002/pip.2425.

[28] *International Electrotechnical Commission (IEC). In Photovoltaic Devices; Procedures for Temperature and Irradiance Corrections to Measure I-V Characteristics*, IEC Standard-60891, 2009.

[29] R. Rüther, A. Montenegro, C. Zomer, I. Santos, L. Nascimento, and P. Grabolle, "Estádios Solares. Opçao sustentável para a copa de 2014 no Brasil. (Relatório Final)," Instituto Ideal/Universidade Federal de Santa Catarina (UFSC), Florianópolis, Brazil, Tech. Rep. GTZ 2007.2189.4-001.00, 2010, pp. 1–58.

[30] *Avaliacão do Desempenho da Usina Fotovoltaica do Mineirão-Maio a Novembro (Presentation)*, Companhia Energética de Minas Gerais (CEMIG), Belo Horizonte, Brazil, 2014, pp. 1–30.

[31] *Martifier Solar. Central Fotovoltaica do Estádio do Mineirão (1.42 MWp)-Projeto de Execucão; Infraestruturas Elétricas, Cálculos Justificativos*, Martifer Solar, Oliveira de Frades, Portugal, 2013, p. 49.

[32] *Photovoltaic Devices-Part 9: Solar Simulator Performance Requirements*, IEC Standard-60904-9, 2007.

[33] D. Atsu, I. Seres, M. Aghaei, and I. Farkas, "Analysis of long-term performance and reliability of PV modules under tropical climatic conditions in sub-saharan," *Renew. Energy*, vol. 162, pp. 285–295, Dec. 2020, doi: 10.1016/j.renene.2020.08.021.

[34] Y. H. Hishikawa, M. Ohshima, K. Higa, and T. Yamagoe, "Precise determination of the STC I-V curves by wide-range linear extrapolation of outdoor I-V curves on partly sunny days," in *Proc. 32th EU PV Solar Energy Conf. Exhib.*, Munich, Germany, Jun. 2016, pp. 1–6.

[35] Y. Hishikawa, T. Doi, M. Higa, K. Yamagoe, and H. Ohshima, "Precise outdoor PV module performance characterization under unstable irradiance," *IEEE J. Photovolt.*, vol. 6, no. 5, pp. 1221–1227, Sep. 2016, doi: 10.1109/JPHOTOV.2016.2571620.

[36] M. Kusko, V. Saly, and M. Perny, "Comparison of translation techniques by PV module diagnostics at outdoor conditions," *Electroteh. Electron. Autom.*, vol. 61, no. 2, pp. 45–50, 2013.

[37] J. Montes-Romero, M. Torres-Ramírez, J. D. L. Casa, A. Firman, and M. Cáceres, "Software tool for the extrapolation to standard test conditions (STC) from experimental curves of photovoltaic modules," in *Proc. Technol. Appl. Electron. Teach. (TAEE)*, Seville, Spain, Jun. 2016, pp. 1–7, doi: 10.1109/TAEE.2016.7528252.

[38] *Guide To Interpreting I-V Curve Measurements of PV Arrays*, Standard PVA-600-1, 2011, pp. 1–60.

[39] K. Emery, "Uncertainty analysis of certified photovoltaic measurements at the national renewable energy laboratory," Nat. Renew. Energy Lab. (NREL), Golden, CO, USA, Tech. Rep. NREL/TP-520-45299, 2009, p. 66.

[40] C. Hansen and C. Martin, "Photovoltaic system modeling: Uncertainty and sensitivity analyses," Sandia Nat. Laboratories, Albuquerque, NM, USA, Tech. Rep. SAND2015-6700, 2015, p. 60.

[41] *Joint Committee for Guides in Metrology (JCGM). Evaluation of Measurement Data: Guide to the Expression of Uncertainty in Measurement (GUM)*, Standard JCGM 100 2008.

[42] M. Richter, K. D. Brabandere, J. Kalisch, T. Schmidt, and E. Lorenz, "Best practice guide on uncertainty in PV modelling," Performance plus WP2 Deliverable D2.4, Univ. Oldenburg, Oldenburg, Germany, Tech. Rep. D2.4, 2015.

[43] *Crystalline Silicon Photovoltaic (PV) Array-On-site Measurements of I-V Characteristics*, IEC Standard 61829, 1995.

[44] J. Dubard, R. Filtz, and V. Cassagne, "Photovoltaic module performance measurements traceability: Uncertainties survey," *Measurement*, vol. 51, pp. 451–456, May 2014, doi: 10.1016/j.measurement.2014.02.025.

[45] *Solmetric White Paper: Winning PV Contracts With I-V Curve Testing*, Solmetric Corp., Sebastopol, CA, USA, 2011.

[46] C. Podewils and M. Bosworth, "The learning curve IV curve tracers are increasing in precision and ease of use, but there's still no perfect product," *Photon–Photovoltaic Mag.*, no. 8, pp. 52–71, 2012.

[47] V. Fakhfouri, "Uncertainty calculation in PV measurement, simulator's and E-loads calibration," Pasan Meas. Syst./Meyer Burger Group, Neuchâtel, Switzerland, Tech. Rep., 2014.

[48] V. Fakhfouri, W. Herrmann, W. Zaaiman, C. Dreier, C. Droz, K. Morita, and L. Johnson, "Uncertainty assessment of PV power measurement in industrial environments," in *Proc. 26th Eur. Photovolt. Sol. Energy Conf. Exhib.*, Hamburg, Germany, 2011, pp. 3408–3412.

[49] J. T. Nakos, "Uncertainty analysis of thermocouple measurements used in normal and abnormal thermal environment experiments at Sandia's radiant heat facility and Lurance canyon burn site," Sandia Nat. Lab., Albuquerque, NM, USA, Tech. Rep. SAND2004-1023, 2004, p. 82.

[50] *Fluke ScopeMeter 190 Series II; User's Manual*, Fluke Corp., Everett, WA, USA, 2011, p. 158.

[51] *Photovoltaics System Performance Monitoring-Guidelines for Measurement Data Exchange and Analysis*, IEC Standard 61724, IEC, Geneva, Switzerland, 1998.

[52] *Analysis of Long-Term Performance of PV Systems: Different Data Resolution for Different Purposes*, Standard IEA-PVPS T13-05:2014, 2014, p. 60.
[53] R. Nolasco, L. Monteiro, V. Mendes, and A. Arcanjo, "Análise preliminar do desempenho de micro usinas fotovoltaicas instaladas na regiao metropolitana de Belo Horizonte," in *Proc. 6th Congresso Brasileiro De Energia Sol. (VI CBENS)*, Belo Horizonte, Brazil, 2016, p. 8.
[54] D. C. Jordan and S. R. Kurtz, "Photovoltaic degradation rates–An analytical review," *Prog. Photovolt., Res. Appl.*, vol. 21, no. 1, pp. 12–29, Jan. 2013, doi: 10.1002/pip.1182.
[55] D. C. Jordan, S. R. Kurtz, K. VanSant, and J. Newmiller, "Compendium of photovoltaic degradation rates," *Prog. Photovolt., Res. Appl.*, vol. 24, no. 7, pp. 978–989, Jul. 2016, doi: 10.1002/pip.2744.
[56] D. Dirnberger, "Uncertainty in PV module measurement—Part II: Verification of rated power and stability problems," *IEEE J. Photovolt.*, vol. 4, no. 3, pp. 991–1007, May 2014, doi: 10.1109/JPHOTOV.2014.2307158.
[57] J. Robledo, J. Leloux, E. Lorenzo, and C. A. Gueymard, "From video games to solar energy: 3D shading simulation for PV using GPU," *Sol. Energy*, vol. 193, pp. 962–980, Nov. 2019, doi: 10.1016/j.solener.2019.09.041.
[58] F. Martínez-Moreno, J. Muñoz, and E. Lorenzo, "Experimental model to estimate shading losses on PV arrays," *Sol. Energy Mater. Sol. Cells*, vol. 94, no. 12, pp. 2298–2303, Dec. 2010, doi: 10.1016/j.solmat.2010.07.029.
[59] A. Maki and S. Valkealahti, "Effect of photovoltaic generator components on the number of MPPs under partial shading conditions," *IEEE Trans. Energy Convers.*, vol. 28, no. 4, pp. 1008–1017, Dec. 2013, doi: 10.1109/tec.2013.2274280.
[60] Y.-M. Saint-Drenan and T. Barbier, "Data-analysis and modelling of the effect of inter-row shading on the power production of photovoltaic plants," *Sol. Energy*, vol. 184, pp. 127–147, May 2019, doi: 10.1016/j.solener.2019.03.086.
[61] P. R. Satpathy, S. Jena, and R. Sharma, "Power enhancement from partially shaded modules of solar PV arrays through various interconnections among modules," *Energy*, vol. 144, pp. 839–850, Feb. 2018, doi: 10.1016/j.energy.2017.12.090.

LUÍS GUILHERME MONTEIRO received the degree in control and automation engineering from the Pontifícia Universidade Católica de Minas Gerais (PUC Minas), in 2002, the master's degree in energy, in the specialty Photovoltaic Systems, from the University of São Paulo (USP), in 2005, and the Ph.D. degree in electrical engineering, in the specialty photovoltaic systems, from the Federal University of Minas Gerais (UFMG), in 2016. He has worked as a Researcher with the Photovoltaic Systems Laboratory (LSF), Institute of Energy and Environment (IEE), USP, from 2003 to 2005, the Brazilian Center for Development of Thermal Solar Energy (GREEN Solar), from March 1998 to December 2002 and February 2005 to October 2009, and the Laboratory of Solar Materials of the Foundation Technological Center of Minas Gerais (CETEC), from March 2011 to December 2011. He is currently an Adjunct Professor IV with the Polytechnic Institute (IPUC), Pontifical Catholic University of Minas Gerais (PUC Minas), a Professor of the Graduate Course (Lato-Sensu) in renewable energy sources: generation, operation and integration; subject photovoltaic systems, and a Postdoctoral Resident of the Graduate Program in Electrical Engineering (PPGEE), Federal University of Minas (UFMG). In this same institution, he also works as a Researcher with the Tesla Laboratory (Power Engineering) and the Energy Conversion and Control Laboratory (LCCE) of the Electrical Engineering Department of the Engineering School, UFMG. He has experience in the energy area, with an emphasis on renewable energy, acting mainly in the following themes: photovoltaic solar energy (isolated systems and systems connected to the electric grid-distributed generation/generation in large plants) and thermal solar energy (solar radiation and flat collectors).

WILSON NEGRÃO MACÊDO received the degree and the master's degree in electrical engineering from the Federal University of Pará, in 1999 and 2002, respectively, and the Ph.D. degree in energy from the University of São Paulo, in 2006. He has worked with the Laboratory of Photovoltaic Systems, Institute of Electrotechnics and Energy, University of São Paulo, from 2002 to 2006. He is currently an Associate Professor II with the Institute of Technology, Federal University of Pará. He also develops research in the field of photovoltaic solar energy and hybrid systems with the Group of Studies and Development of Energy Alternatives of the Federal University of Pará (GEDAE/UFPA), where he coordinates the Laboratory of Photovoltaic Systems, and is also a Researcher at the Research Group on Innovation, Development and Adaptation of Sustainable Technologies–GPIDATS–IDSM-OS. He has experience in the area of electrical engineering, with an emphasis on electrical power systems, acting mainly in the following themes: distributed generation, solar photovoltaic energy, connection to the low voltage electrical networks, renewable energy, and attendance of isolated localities.

RENATO L. CAVALCANTE received the degree in electrical engineering and the master's degree in electrical engineering from the Federal University of Pará, in 2011 and 2014, respectively. He is currently a permanent Professor with the Federal University of Pará and the Scholarship holder of the Study Groups and Development of Energy Alternatives. He has experience in electrical engineering, with an emphasis on photovoltaic systems, working mainly on the following topics: grid-connected photovoltaic systems, renewable energy, solar energy, monitoring systems, and power generation.

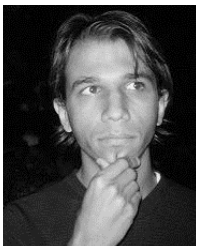

WILSON BRAGA JÚNIOR received the degree in energy engineering from the Pontifical Catholic University of Minas Gerais, in 2011, and the master's degree in renewable energies from the Federal University of Pará, in 2014. He has been a Professor in electrical and civil engineering disciplines with UNIUBE, since 2014. He has participated in several projects related to photovoltaic solar energy with the Group of Studies and Development of Energy Alternatives, Federal University of Pará. He has a technical course in industrial mechanics from the Federal Center of Technological Education of Minas Gerais, in 2005. He was a Professor of technical courses at ASA College from 2010 to 2012. He made scientific initiation in a project of thermoelectric generation for steel industries in 2010. He received the Outstanding Academic Awards and the Gold Medal during his degree in energy engineering.

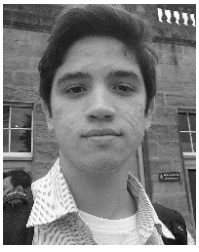

PEDRO FERREIRA TORRES received the degree in electrical engineering and the master's degree in electrical engineering from the Federal University of Pará (UFPA), in 2017 and 2019, respectively. He carried out an exchange with the Modality Sandwich Graduation in Electrical Engineering, State University of North Carolina (NCSU), USA, where he participated in the development of a project in the area of power electronics, helping in the construction of power converters. He currently carries out research activities at the Photovoltaic Systems Laboratory, Institute of Energy and Environment (IEE), University of São Paulo (USP). He is interested in mini grids, distributed generation, power electronics, and power systems, applied to the development of renewable energies.

THIAGO R. BRITO (Member, IEEE) received the degrees in science and technology and energy engineering from the Federal University of ABC, in 2013 and 2015, respectively, and the master's degree in electrical engineering from UFPA, in 2018. He was a part of the Energy Alternatives Study and Development Group (GEDAE), UFPA. He has experience in energy engineering, with an emphasis on renewable energy sources and photovoltaic engineering.

MÁRCIO MELQUIADES SILVA received the degree in electrical engineering from the Pontifical Catholic University of Minas Gerais, in 1993, the degree in pedagogical training of teachers from the Minas Gerais Education for Work Foundation, in 1997, the master's degree in technology from the Federal Center for Technological Education of Minas Gerais, in 2004, and the Ph.D. degree in electrical engineering from UFMG, in 2015. He teaches basic technical and technological education at the Federal Center for Technological Education of Minas Gerais. He has experience in the area of electrical engineering, with an emphasis on the design and execution of electrical installations and medium voltage substations.

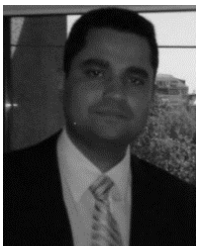

BRUNO MARCIANO LOPES received the degree in electrical engineering and the master's degree in electrical engineering from the Federal University of Minas Gerais, in 2003 and 2006, respectively. He has experience in the field of electrical engineering, with an emphasis on power electronics, acting mainly on the following themes: voltage sinking, power quality, dynamic voltage restorer, loss calculation, and converter design. He has been working with the CEMIG's Energy Alternatives Management, since 2006, where he works in the technical supervision of the Minas Gerais Energy Balance, prospective studies on energy, analysis of alternative energy sources and technologies, and distributed generation and manages research and development projects related to energy alternatives. He currently manages research projects and the implementation of projects in the area of photovoltaic solar generation, the main ones being Research and Development 470, referring to the USF of Sete Lagoas, Mineirão Solar, and projects of Strategic Call 13 of ANEEL's Research and Development Program.

JULIANO M. FRAGA received the degree in information systems from the Faculdades Integradas do Oeste de Minas (FADOM), in 2004, and the degree in bioenergetic engineering from Universidade FUMEC, in 2016. He is currently an Industrial Technician with CEMIG Geracão e Transmissão.

DANILO DERICK ALVES received the bachelor's and master's degrees in electrical engineering from the Federal University of Minas Gerais, in 2006 and 2010, respectively. He is currently a Technology and Standardization Engineer with CEMIG D. He has experience in the area of electrical engineering.

OTÁVIO A. CHASE (Senior Member, IEEE) received the B.Sc. degree in computer engineering, with an emphasis on electronic systems, from the Institute of Higher Studies of the Amazonia (IESAM), in 2007, and the M.Sc. and D.Sc. degrees in electrical engineering, in the area of electrical energy systems, from the Federal University of Pará (UFPA), in 2009 and 2018, respectively. He has been an Adjunct Professor III at the Federal Rural University of the Amazonia (UFRA); a member of the Cyberphysical Systems Laboratory, ICIBE/UFRA, since 2010; a Senior Member of the IEEE, Section: Instrumentation and Measurement; and a Full Member of the Pará Academy of Sciences (APaCi). Since 2000, he works in projects of research, development, and innovation in embedded electronic systems, cyberphysical systems, mechatronics, education in engineering, environmental technologies, and renewable energy.

WALLACE C. BOAVENTURA (Member, IEEE) received the degree in electrical engineering and the master's degree in electrical engineering from the Federal University of Minas Gerais, in 1987 and 1990, respectively, and the Ph.D. degree in electrical engineering from the State University of Campinas, in 2002, with an internship at the University of Toronto (UofT). He is currently a Full Professor with the Federal University of Minas Gerais. He has experience in electrical engineering, emphasizing electricity transmission, electricity distribution, working mainly on the following topics: energy systems, electromagnetic compatibility, atmospheric discharges, high voltage, and signal processing applications.